SN 2002cv: a heavily obscured Type Ia supernova

N. Elias-Rosa,[1,2]★ S. Benetti,[2] M. Turatto,[2] E. Cappellaro,[2] S. Valenti,[3]
A. A. Arkharov,[4] J. E. Beckman,[5] A. Di Paola,[6] M. Dolci,[7] A. V. Filippenko,[8]
R. J. Foley,[8] K. Krisciunas,[9] V. M. Larionov,[4,10] W. Li,[8] W. P. S. Meikle,[11]
A. Pastorello,[12] G. Valentini[7] and W. Hillebrandt[1]

[1]*Max-Planck-Institut für Astrophysik, Karl-Schwarzschild-Str. 1, D-85748 Garching bei München, Germany*
[2]*INAF – Osservatorio Astronomico di Padova, vicolo dell'Osservatorio 5, I-35122 Padova, Italy*
[3]*European Southern Observatory, Karl-Schwarzschild-Str. 2, D-85748 Garching bei München, Germany*
[4]*Main (Pulkovo) Astronomical Observatory of the RAS, St Petersburg, Russia*
[5]*Instituto de Astrofísica de Canarias, C/ Vía Láctea s/n, E-38200 La Laguna, Tenerife, Spain*
[6]*INAF – Osservatorio Astronomico di Roma, via Frascati 33, Monteporzio Catone, I-00040 Roma, Italy*
[7]*INAF – Osservatorio Astronomico di Collurania, via M. Maggini, I-64100 Teramo, Italy*
[8]*Department of Astronomy, University of California, Berkeley, CA 94720-3411, USA*
[9]*Department of Physics, Texas A&M University, College Station, TX 77843-4242, USA*
[10]*Astronomical Institute of St. Petersburg State University, St Petersburg,Russia*
[11]*Astrophysics Group, Imperial College London, Blackett Laboratory, Prince Consort Road, London SW7 2AZ*
[12]*Astrophysics Research Centre, Queen's University Belfast, Belfast BT7 1NN*

ABSTRACT

We present *VRIJHK* photometry, and optical and near-infrared spectroscopy, of the heavily extinguished Type Ia supernova (SN Ia) 2002cv, located in NGC 3190, which is also the parent galaxy of the SN Ia 2002bo. SN 2002cv, not visible in the blue, has a total visual extinction of 8.74 ± 0.21 mag. In spite of this, we were able to obtain the light curves between -10 and $+207$ d from the maximum in the *I* band, and also to follow the spectral evolution, deriving its key parameters. We found the peak *I*-band brightness to be $I_{max} = 16.57 \pm 0.10$ mag, the maximum absolute *I* magnitude to be $M_I^{max} = -18.79 \pm 0.20$, and the parameter $\Delta m_{15}(B)$ specifying the width of the *B*-band light curve to be 1.46 ± 0.17 mag. The latter was derived using the relations between this parameter and $\Delta m_{40}(I)$ and the time-interval $\Delta t_{max}(I)$ between the two maxima in the *I*-band light curve. As has been found for previously observed, highly extinguished SNe Ia, a small value of 1.59 ± 0.07 was obtained here for the ratio R_V of the total-to-selective extinction ratio for SN 2002cv, which implies a small mean size for the grains along the line of sight towards us. Since it was found for SN 2002bo a canonical value of 3.1, here we present a clear evidence of different dust properties inside NGC 3190.

Key words: supernovae: general – supernovae: individual: SN 2002cv – dust, extinction.

1 INTRODUCTION

Type Ia supernovae (SNe Ia) are believed to result from the explosion of white dwarfs when they reach the Chandrasekhar limit after accreting mass from a nearby companion star. The overall homogeneity and the small brightness dispersion at maximum qualify SNe Ia as the most powerful tools for measuring cosmological distances (see Filippenko 2005 for a comprehensive review). Over the last decade, a number of studies have been dedicated to the detailed analysis of light curves of SNe Ia and the determination of the peak magnitudes (e.g. Hamuy et al. 1996a; Riess, Press & Kirshner 1996; Perlmutter et al. 1997; Phillips et al. 1999; Prieto, Rest & Suntzeff 2006), host-galaxy extinctions (e.g. Krisciunas et al. 2004b; Wang 2005;

Elias-Rosa et al. 2006; Krisciunas et al. 2006), statistical analysis of spectral properties (e.g. Benetti et al. 2005; Mazzali et al. 2005; Branch et al. 2006; Hachinger, Mazzali & Benetti 2006; Mazzali et al. 2007), and progenitor and explosion models (Hillebrandt & Niemeyer 2000; Gamezo, Khokhlov & Oran 2005; Röpke et al. 2006, 2007; Nomoto et al. 2007). All these works have been possible only due to intensive campaigns of observation and accurate calibration of nearby SNe Ia (e.g. Suntzeff 1996; Krisciunas et al. 2003; Benetti et al. 2004; Jha et al. 2006; Pastorello et al. 2007b).

A crucial factor to be considered in the calibration of SNe is the extinction occurring inside the host galaxy, which is generally derived by measuring the reddening and adopting a standard value for the total-to-selective absorption ratio, $R_V = A_V E(B - V)$. On the other hand, it is well known that R_V depends on the nature of interstellar dust and varies even with the line of sight inside

★ E-mail: nelias@mpa-garching.mpg.de

the Galaxy from $R_V \approx 2$ to ~ 5.5 (Fitzpatrick 2004; Geminale & Popowski 2005) with an average value of $R_V = 3.1$ (Savage & Mathis 1979; Seaton 1979). Whereas very little is known for other galaxies, usually it is assumed that the dust has the same average properties as in the Galaxy. In most cases, measurements along the line of sight to the SNe show canonical values of $R_V = 3.1$ (e.g. SN 1994D – Patat et al. 1996, SN 2002bo – Benetti et al. 2004, SN 2004eo – Pastorello et al. 2007b), but for a few SNe these measurements show evidence for extremely low values of R_V. In particular, SN Ia 1999cl (Krisciunas et al. 2006) was reddened by dust with $R_V = 1.55 \pm 0.08$. For the core-collapse SN 2002hh (Pozzo et al. 2006), a two-component extinction model has been proposed to match coeval spectral templates with $A_V = 3.3$ mag, $R_V = 1.1$ and with $A_V = 1.7$ mag, $R_V = 3.1$. For another heavily extinguished SN Ia, SN 2003cg, Elias-Rosa et al. (2006) found $R_V = 1.80 \pm 0.19$ and $E(B - V) = 1.33 \pm 0.11$ mag. Given the dependence of R_V on the dust properties, the dust along the line of sight to these SNe seems to have very small grain size. An alternative explanation calls for the contamination by unresolved light echo from circumstellar dust (Wang 2005). The growing number of SNe Ia associated with dust clouds with unusual properties is of interest not only in the context of SN calibration, but also for the debate on progenitor scenarios (Patat et al. 2007).

In this paper, we discuss the case of SN 2002cv, one of the most-obscured SNe ever observed (Di Paola et al. 2002). It was discovered in the spiral galaxy NGC 3190 (heliocentric velocity of 1271 km s^{-1}) on 2002 May 13.7 (UT dates are used throughout this paper) by Larionov & Arkharov (2002) during the campaign of monitoring of SN 2002bo, an SN Ia extensively studied by Benetti et al. (2004) and Krisciunas et al. (2004b). The new source was found 18 arcsec west and 10 arcsec north of the galactic nucleus ($\alpha = 10^h18^m03^s68$, $\delta = +21°50'06''20$, J2000.0) projected on the galaxy dust lane (Fig. 1). An early optical spectrum (Turatto et al. 2002) showed a very red continuum with almost no signal bluewards of 600 nm, which was attributed to very high extinction. Infrared (IR) spectra taken at the United Kingdom Infrared Telescope (UKIRT) on May 22.3 and 23.3 (Meikle & Mattila 2002) suggested that SN 2002cv was an SN Ia similar to the bright SN 1991T (Filippenko 1997; Filippenko et al. 1992a). This classification was confirmed by Filippenko et al. (2002). Meikle & Mattila (2002) also estimated that

the value of A_V towards SN 2002cv actually exceeded 6 mag, the highest extinction ever recorded for an SN Ia.

Here, we present a wide set of photometric data obtained worldwide for SN 2002cv along with selected spectroscopic observations. The description of the data reduction and the analysis of the light curves are given in Section 2. Section 3 presents the optical and IR spectra. In Section 4, we discuss the reddening, while in Section 5 we derive the main parameters of the SN using empirical relations both from the literature and from that derived here. We conclude with a summary of the results (Section 6).

2 PHOTOMETRY

2.1 Data acquisition and reduction

The fact that another SN Ia, SN 2002bo, exploded in the same galaxy a few months before SN 2002cv, makes available pre-discovery optical and near-IR (NIR) data and hence templates for photometric measurements via image subtraction. SN 2002cv was observed for seven months, from day -10.7 to $+205.9$ relative to I-band maximum light. Here, we present the data collected by four different teams: University of California, Berkeley (USA), Imperial College (UK), Padova Observatory (INAF, Italy) and Teramo Observatory (INAF, Italy). The following is the list of a total of nine different instrument configurations that were used.

(i) 1-m Nickel telescope (Lick Observatory, Mt Hamilton, California, USA), equipped with a SITe thinned CCD (1024 × 1024 pixel, 0.28 arcsec pixel^{-1}, field of view 6.3 × 6.3 arcmin^2).

(ii) 0.72-m Teramo–Normale Telescope (Terano, Italy), equipped with a TK512CB1-1 CCD (512 × 512 pixel, 0.46 arcsec pixel^{-1}, field of view 3.92 × 3.92 arcmin^2).

(iii) 0.76-m Katzman Automatic Imaging Telescope (Lick Observatory, Mt Hamilton, California, USA), equipped with a SITe AP7 CCD (512 × 512 pixel, 0.8 arcsec pixel^{-1}, field of view 6.7 × 6.7 arcmin^2).

(iv) 1.82-m Copernico telescope of Mt Ekar (Asiago, Italy), equipped with AFOSC (thinned TEK CCD, 1024 × 1024 pixel, 0.473 arcsec pixel^{-1}, field of view 8.14 × 8.14 arcmin^2).

(v) 3.6-m ESO/NTT telescope (La Silla, Chile), equipped with EMMI (Tektronix TK1034 CCD, 1024 × 1024 pixel; blue arm
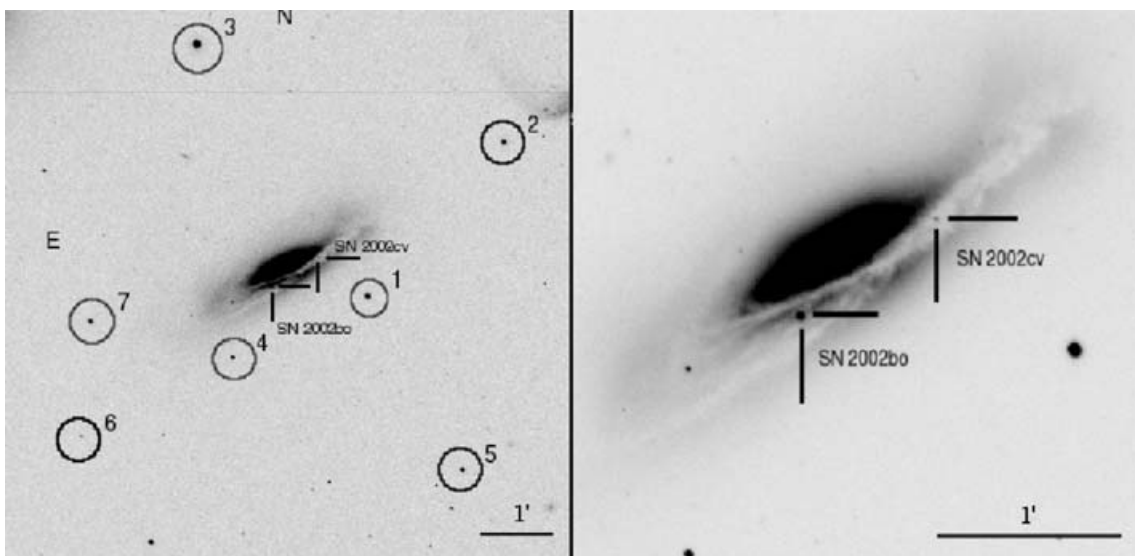

Figure 1. *R*-band image of SN 2002cv in NGC 3190 taken with the 2.5-m Isaac Newton Telescope + WFC on 2002 June 27 (field of view $\sim 8 \times 8$ arcmin^2). SN 2002bo and the local sequence stars are also indicated (see Table 1).

Table 1. Adopted magnitudes for the local sequence stars, coded as in Fig. 1 (see Section 2.1).

Star	*V*	*R*	*I*	*J*	*H*	*K*
1	14.42 ± 0.02	13.99 ± 0.03	13.58 ± 0.01	13.05 ± 0.01	12.71 ± 0.01	12.67 ± 0.01
2	14.33 ± 0.04	13.93 ± 0.04	13.57 ± 0.02	–	–	–
3	12.40 ± 0.05	12.05 ± 0.05	11.68 ± 0.05	–	–	–
4	17.20 ± 0.02	16.35 ± 0.03	15.65 ± 0.03	14.83 ± 0.01	14.20 ± 0.01	14.12 ± 0.01
5	15.64 ± 0.04	15.26 ± 0.04	14.91 ± 0.01	–	–	–
6	17.90 ± 0.02	17.51 ± 0.05	17.05 ± 0.10	–	–	–
7	14.92 ± 0.01	14.49 ± 0.01	14.06 ± 0.01	–	–	–

0.37 arcsec pixel^{-1}, field of view 6.2 × 6.2 arcmin^2; red arm 0.167 arcsec pixel^{-1}, field of view 9.1 × 9.9 arcmin^2).

(vi) 2.5-m Isaac Newton Telescope (INT) (Roque de los Muchachos Observatory, La Palma, Spain), equipped with Wide Field Camera (four thinned EEV CCDs, 2048 × 4096 pixel, 0.33 arcsec pixel^{-1}, field of view 34 × 34 arcmin^2).

(vii) 1.0-m Jacob Kapteyn Telescope (Roque de los Muchachos Observatory, La Palma, Spain), equipped with JAG (SITe2 CCD, 2048 × 2048 pixel, 0.33 arcsec pixel^{-1}, field of view 10 × 10 arcmin^2).

(viii) 3.6-m ESO/NTT Telescope (La Silla, Chile), equipped with SofI (NIR HgCdTe Hawaii array, 1024 × 1024 pixel, 0.288 arcsec pixel^{-1}, field of view 4.94 × 4.94 arcmin^2).

(ix) 1.08-m AZT-24 telescope (Campo Imperatore, Italy), equipped with SWIRCAM (NIR HgCdTe PICNIC array, 256 × 256 pixel, 1.04 arcsec pixel^{-1}, field of view 4.4 × 4.4 arcmin^2).

The photometric observations were processed using IRAF[1] routines with the standard recipe for CCD images (trimming, overscan, bias, and flat-field corrections). For the NIR bands, we also performed sky image subtraction, as well as image co-addition to improve the signal-to-noise ratio.

In all cases, because of the strong luminosity gradient at the SN position, we made use of the template-subtraction technique in order to measure the SN magnitudes (Filippenko et al. 1986). Image subtraction was performed using the ISIS program (Alard 2000). As reference images (templates) of the host galaxy, we selected those taken about two months before the discovery of SN 2002cv with the Asiago 1.82-m Copernico telescope + AFOSC on 2002 March 21 and the AZT-24 Telescope + SWIRCAM on 2002 March 28, for the optical and NIR bands, respectively. After geometrical and photometric registration of the two images (target image and template) and the degradation of the image with the best seeing to match the worst one, the template was subtracted from the target image. Hereafter, the instrumental magnitude of the SN was measured with the point spread function (PSF) fitting technique using the DAOPHOT package on the subtracted image. Reference stars in the SN field (see Fig. 1) were also measured using the IRAF PSF fitting routine on the original image.

In order to calibrate the instrumental magnitudes on to a standard photometric system, we used the specific colour-term equations for each of the various instrumental configurations. For the optical bands, these were derived from observations during photometric nights of several standard fields (Landolt 1992). In turn,

---

[1] IRAF is written and supported by the IRAF programming group at the National Optical Astronomy Observatories (NOAO) in Tucson, Arizona, which are operated by the Association of Universities for Research in Astronomy (AURA), Incorporated, under cooperative agreement with the National Science Foundation.
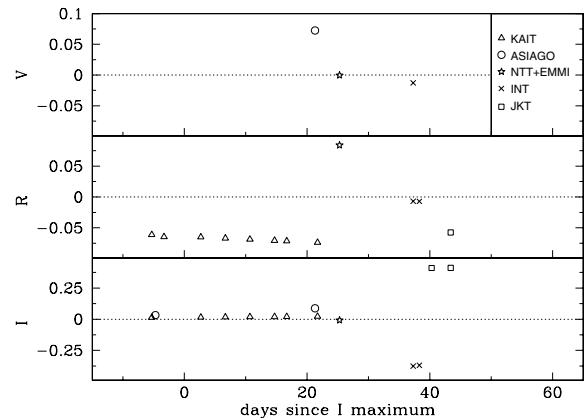

Figure 2. Summary of the S-corrections derived for the *VRI* bands of the different instruments (see the legend) at early times. These corrections have been added to the first-order corrected SN 2002cv magnitudes to convert them to the standard system. The dotted line shows the zero correction.
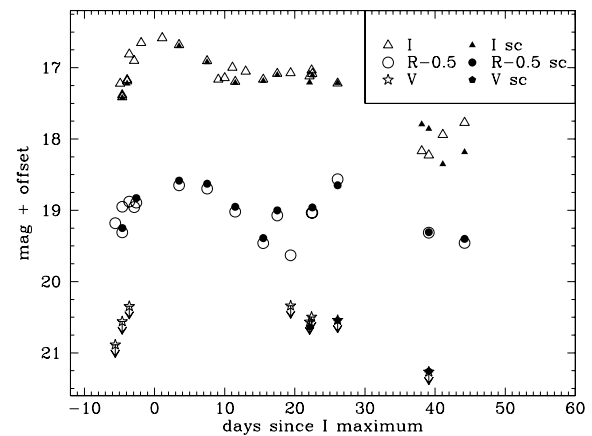

Figure 3. Comparison between the original *VRI* light curves (empty symbols) of SN 2002cv and the corrected ones (filled symbols). Note that we were not able to apply the S-correction to some instruments; 'sc' stands for 'S-corrected'.

the photometric zero-points for non-photometric nights were determined using the magnitudes of the local sequence stars in the SN field (Table 1). For the NIR, because of the small number of standard stars observed each night, we used the average colour terms provided by the telescope teams.

Actually, after the detailed monitoring of SN 2002bo, accurate estimates are available for the magnitudes of a number of local standard stars which are used to calibrate our data (Benetti et al. 2004; Krisciunas et al. 2004b; KAIT observations). The order of the local sequence is that given by Benetti et al. (2004; see their fig. 1

Table 2. S-correction to be added to the data of SN 2002cv in Table 3.

Date	JD (2 400 000.00)	Phase[a] (d)	V	R	I	Instrument
15/05/02	524 09.75	−5.3	–	−0.061(0.009)	0.014(0.011)	KAIT
15/05/02	524 10.40	−4.7	–	–	0.033(0.019)	EKAR
17/05/02	524 11.75	−3.3	–	−0.064(0.009)	–	KAIT
23/05/02	524 17.75	2.7	–	−0.065(0.009)	0.016(0.011)	KAIT
27/05/02	524 21.75	6.7	–	−0.067(0.009)	0.017(0.011)	KAIT
31/05/02	524 25.75	10.7	–	−0.069(0.009)	0.018(0.011)	KAIT
4/06/02	524 29.75	14.7	–	−0.071(0.009)	0.020(0.011)	KAIT
6/06/02	524 31.75	16.7	–	−0.071(0.009)	0.020(0.011)	KAIT
10/06/02	524 36.37	21.3	0.073(0.044)	–	0.088(0.019)	EKAR
11/06/02	524 36.75	21.7	–	−0.074(0.009)	0.022(0.011)	KAIT
14/06/02	524 40.39	25.3	−0.001(0.017)	0.084(0.019)	-0.007(0.012)	EMMI
26/06/02	524 52.40	37.3	−0.013(0.003)	−0.007(0.001)	-0.376(0.053)	INT
27/06/02	524 53.42	38.3	–	−0.007(0.001)	-0.369(0.053)	INT
29/06/02	524 55.43	40.3	–	–	0.411(0.028)	JKT
2/07/02	524 58.45	43.4	–	−0.057(0.006)	0.412(0.028)	JKT

[a]Relative to I_{max} (JD = 2 452 415.09).
Notes. KAIT = 0.76-m Katzman Automatic Imaging Telescope + CCD, 0.80 arcsec pixel^{-1}; EKAR = 1.82-m Copernico telescope + AFOSC, 0.47 arcsec pixel^{-1}; EMMI = 3.6-m ESO NTT + EMMI, 0.167 arcsec pixel^{-1}; INT = 2.5-m Isaac Newton Telescope + WFC, 0.33 arcsec pixel^{-1}; JKT = 1.0-m Jacob Kapteyn Telescope + JAG, 0.33 arcsec pixel^{-1}.

Table 3. Original optical photometry of SN 2002cv.

UT date	JD (2 400 000.00)	Phase[a] (d)	V	R	I	Instrument
14/05/02	524 08.75	−6.3	⩾ 20.97	19.81(0.18)	–	N1mT
14/05/02	524 09.37	−5.7	⩾ 20.48	–	17.23(0.14)	TNT
15/05/02	524 09.74	−5.4	⩾ 20.69	19.62(0.27)	17.45(0.11)	N1mT
15/05/02	524 09.75	−5.3	–	19.79(0.26)	17.48(0.03)	KAIT
15/05/02	524 10.39	−4.7	–	–	17.18(0.44)	TNT
15/05/02	524 10.40	−4.7	–	–	17.28(0.04)	EKAR
16/05/02	524 10.74	−4.4	⩾ 20.50	19.54(0.06)	16.89(0.11)	N1mT
16/05/02	524 11.41	−3.7	–	19.42(0.68)	16.69(0.18)	TNT
17/05/02	524 11.75	−3.3	–	19.35(0.09)	–	KAIT
17/05/02	524 12.38	−2.7	–	–	16.65(0.44)	TNT
20/05/02	524 15.39	0.3	–	–	16.67(0.09)	TNT
23/05/02	524 17.75	2.7	–	19.30(0.25)	16.84(0.12)	KAIT
27/05/02	524 21.75	6.7	–	19.34(0.18)	17.04(0.14)	KAIT
28/05/02	524 23.37	8.3	–	–	17.25(0.12)	TNT
29/05/02	524 24.33	9.2	–	–	17.23(0.10)	TNT
30/05/02	524 25.36	10.3	–	–	17.24(0.10)	TNT
31/05/02	524 25.75	10.7	–	19.65(0.07)	17.33(0.30)	KAIT
1/06/02	524 27.28	12.2	–	–	17.19(0.07)	TNT
4/06/02	524 29.75	14.7	–	20.12(0.16)	17.31(0.56)	KAIT
6/06/02	524 31.75	16.7	–	19.72(0.12)	17.24(0.46)	KAIT
8/06/02	524 33.70	18.6	⩾ 20.46	20.27(0.12)	17.15(0.14)	N1mT
10/06/02	524 36.37	21.3	⩾ 20.65	–	17.20(0.02)	EKAR
11/06/02	524 36.71	21.6	⩾ 20.65	19.65(0.16)	17.08(0.10)	N1mT
11/06/02	524 36.75	21.7	–	19.62(0.20)	17.25(0.24)	KAIT
14/06/02	524 40.39	25.3	⩾ 20.58	19.18(0.08)	17.22(0.02)	EMMI
26/06/02	524 52.40	37.3	–	20.09(0.08)	18.16(0.05)	INT
27/06/02	524 53.42	38.3	⩾ 21.39	20.08(0.11)	18.33(0.06)	INT
29/06/02	524 55.43	40.3	–	–	17.85(0.30)	JKT
2/07/02	524 58.45	43.4	–	20.07(0.23)	17.82(0.07)	JKT
5/12/02	52613.93	198.8	⩾ 23.27	⩾ 23.30	–	N1mT
12/12/02	52620.98	205.9	⩾ 23.85	⩾ 23.41	⩾ 23.28	N1mT

[a]Relative to I_{max} (JD = 2 452 415.09).
Notes. N1mT = 1-m Nickel telescope + CCD, 0.28 arcsec pixel^{-1}; TNT = 0.72-m Teramo–Normale Telescope + CCD, 0.46 arcsec pixel^{-1}; KAIT = 0.76-m Katzman Automatic Imaging Telescope + CCD, 0.80 arcsec pixel^{-1}; EKAR = 1.82-m Copernico telescope + AFOSC, 0.47 arcsec pixel^{-1}; EMMI = 3.6-m ESO NTT + EMMI, 0.167 arcsec pixel^{-1}; INT = 2.5-m Isaac Newton Telescope + WFC, 0.33 arcsec pixel^{-1}; JKT = 1.0-m Jacob Kapteyn Telescope + JAG, 0.33 arcsec pixel^{-1}.

Table 4. S-corrected optical photometry of SN 2002cv.

UT date	JD (2 400 000.00)	Phase[a] (d)	V	R	I	Instrument[b]
14/05/02	524 08.75	−6.3	⩾ 20.97	19.81(0.18)	–	N1mT
14/05/02	524 09.37	−5.7	⩾ 20.48	–	17.23(0.14)	TNT
15/05/02	524 09.74	−5.4	⩾ 20.69	19.62(0.06)	17.45(0.02)	N1mT
15/05/02	524 09.75	−5.3	–	19.73(0.12)	17.49(0.05)	KAIT
15/05/02	524 10.39	−4.7	–	–	17.18(0.12)	TNT
15/05/02	524 10.40	−4.7	–	–	17.32(0.04)	EKAR
16/05/02	524 10.74	−4.4	⩾ 20.50	19.54(0.06)	16.89(0.03)	N1mT
16/05/02	524 11.41	−3.7	–	19.42(0.10)	16.69(0.02)	TNT
17/05/02	524 11.75	−3.3	–	19.28(0.09)	–	KAIT
17/05/02	524 12.38	−2.7	–	–	16.65(0.05)	TNT
20/05/02	524 15.39	0.3	–	–	16.67(0.06)	TNT
23/05/02	524 17.75	2.7	–	19.24(0.08)	16.86(0.06)	KAIT
27/05/02	524 21.75	6.7	–	19.28(0.12)	17.06(0.08)	KAIT
28/05/02	524 23.37	8.3	–	–	17.25(0.04)	TNT
29/05/02	524 24.33	9.2	–	–	17.23(0.04)	TNT
30/05/02	524 25.36	10.3	–	–	17.24(0.02)	TNT
31/05/02	524 25.75	10.7	–	19.58(0.04)	17.35(0.04)	KAIT
1/06/02	524 27.28	12.2	–	–	17.19(0.02)	TNT
4/06/02	524 29.75	14.7	–	20.05(0.16)	17.33(0.28)	KAIT
6/06/02	524 31.75	16.7	–	19.65(0.12)	17.26(0.23)	KAIT
8/06/02	524 33.70	18.6	⩾ 20.46	20.27(0.12)	17.15(0.03)	N1mT
10/06/02	524 36.37	21.3	⩾ 20.72	–	17.29(0.03)	EKAR
11/06/02	524 36.71	21.6	⩾ 20.65	19.65(0.07)	17.08(0.03)	N1mT
11/06/02	524 36.75	21.7	–	19.54(0.20)	17.27(0.12)	KAIT
14/06/02	524 40.39	25.3	⩾ 20.58	19.26(0.08)	17.21(0.02)	EMMI
26/06/02	524 52.40	37.3	–	20.09(0.08)	17.78(0.07)	INT
27/06/02	524 53.42	38.3	⩾ 21.37	20.07(0.03)	17.96(0.06)	INT
29/06/02	524 55.43	40.3	–	–	18.26(0.04)	JKT
2/07/02	524 58.45	43.4	–	20.01(0.23)	18.24(0.08)	JKT
5/12/02	526 13.93	198.8	⩾ 23.27	⩾ 23.30	–	N1mT
12/12/02	526 20.98	205.9	⩾ 23.85	⩾ 23.41	⩾ 23.28	N1mT

[a]Relative to I_{max} (JD = 2 452 415.09). [b]See the note to Table 3 for the telescope coding.

and table 1) with the addition of star number 7 which corresponds to star number 3 of Krisciunas et al. (2004b; see their fig. 1e and table 1). For the NIR magnitudes, we calibrated two stars of the local sequence during photometric nights. The NIR magnitudes of the single star in common with Krisciunas et al. (2004b) agree to better than 0.02 mag.

We also included the data from Di Paola et al. (2002) (see Section 2.2) obtained using the AZT-24 Telescope of the Campo Imperatore Observatory, equipped with the NIR camera SWIRCAM. These data were re-calibrated against our local sequence, while for a few deviant points a new measurement was necessary.

Whereas standard colour corrections properly bring the magnitudes of normal stars to the standard system, it is known that this does not work well for SNe because of their specific spectral energy distribution (SED). This and the differences between bandpasses cause a significant dispersion of the photometric measurements obtained with different instruments. We note that during the follow-up observations of SN 2002cv, we used seven different instruments for the optical and two for the NIR observations.

The accurate SN calibration procedure, usually called S-correction (Suntzeff 2000; Stritzinger et al. 2002; Krisciunas et al. 2003; Pignata et al. 2004; Pignata 2004), requires that the SED of the object and the response curve of the instruments used for the observations are both accurately known.

We computed the S-corrections for the *VRI* bands[2] by using the flux-calibrated spectra of SN 2002cv (Section 3). Since our spectra did not cover all photometric epochs, we completed the spectral data base by adding spectra of unreddened normal SNe Ia such as SN 1992A (Suntzeff 1996), SN 1994D (Patat et al. 1996) and SN 1996X (Salvo et al. 2001), properly reddened to match those of SN 2002cv (see Section 4 for more details).

The corrections for SN 2002cv are in general relatively small (⩽0.1 mag), as seen in Fig. 2 and Table 2, except for the *I* band of the INT and JKT, where the corrections are as high as 0.40 mag. These telescopes use Sloan Gunn *i* and Harris *I* filters, respectively, which differ significantly from the Bessell ones. The SN magnitudes, calibrated using this technique, agree fairly well (Fig. 3). Note that the data from TNT and the Lick Nickel 1-m telescope were not corrected because some of the required instrumental information was not available. In any case, the measurements from these instruments appear to be in good agreement with the S-corrected photometry from other instruments (see Fig. 3).

Uncorrected and S-corrected optical magnitudes are reported in Tables 3 and 4, respectively, and NIR measurements are listed in Table 5. Magnitudes are presented together with their uncertainties,

---

[2] We did not compute the S-correction for NIR bands and for the late-time optical observations because of the lack of suitable spectra.

Table 5. Original NIR photometry of SN 2002cv.

UT date	JD (2 400 000.00)	Phase[a] (d)	J	H	K	Instrument
9/05/02[b]	524 04.39	−10.7	17.05(0.11)	–	16.64(0.11)	AZT
13/05/02[b]	524 08.35	−6.7	15.46(0.01)	14.92(0.02)	14.73(0.05)	AZT
14/05/02[b]	524 09.35	−5.7	15.26(0.01)	14.61(0.02)	14.36(0.03)	AZTDP
15/05/02[b]	524 10.32	−4.8	15.07(0.02)	14.56(0.03)	14.25(0.04)	AZTDP
16/05/02[b]	524 11.36	−3.7	14.90(0.01)	14.44(0.02)	14.21(0.03)	AZT
17/05/02[b]	524 12.38	−2.7	14.89(0.01)	14.34(0.01)	–	AZTDP
20/05/02[b]	524 15.33	0.2	14.75(0.03)	–	13.95(0.03)	AZT
26/05/02[b]	524 21.43	6.3	–	–	14.06(0.04)	AZT
27/05/02[b]	524 22.36	7.3	–	–	14.06(0.05)	AZTDP
28/05/02[b]	524 23.41	8.3	15.37(0.04)	–	–	AZT
29/05/02[b]	524 24.38	9.3	–	14.74(0.02)	–	AZT
30/05/02	524 25.36	10.3	–	–	14.16(0.03)	AZTDP
30/05/02	524 25.42	10.3	15.69(0.07)	–	–	AZT
31/05/02[b]	524 26.41	11.3	15.80(0.02)	–	–	AZTDP
1/06/02[b]	524 27.33	12.2	15.85(0.04)	14.71(0.03)	14.41(0.04)	AZTDP
5/06/02	524 31.36	16.3	16.87(0.08)	14.49(0.04)	14.94(0.07)	AZT
12/06/02	524 38.35	23.3	16.33(0.03)	14.41(0.03)	14.26(0.04)	AZT
16/06/02	524 41.53	26.4	16.04(0.01)	–	14.17(0.01)	SofI
20/06/02	524 46.36	31.3	15.77(0.05)	–	13.95(0.10)	AZT
4/07/02	524 60.33	45.2	–	–	14.40(0.06)	AZT
9/07/02	524 65.33	50.2	15.87(0.09)	–	–	AZT
10/07/02	524 66.33	51.2	–	15.39(0.10)	–	AZT
1/07/02	524 67.32	52.2	–	–	14.89(0.07)	AZT
12/07/02	524 68.33	53.2	16.50(0.10)	–	–	AZT
22/07/02	524 78.30	63.2	–	–	14.25(0.80)	AZT

[a]Relative to I_{max} (JD = 2 452 415.09). [b]Photometric night.

Notes. AZT = 1.08-m AZT-24 + SWIRCAM, 1.04 arcsec pixel^{-1}; AZTDP = data from Di Paola et al. (2002) using the same configuration as AZT; SofI = 3.6-m ESO NTT + SofI, 0.29 arcsec pixel^{-1}.

which were computed as the quadrature sum of the following contributions: the square root of the PSF fitting errors on the subtracted images, calibration errors (rms of the observed magnitudes of the local sequence stars), and errors associated to the S-correction (rms deviation with respect to the low-order polynomial fit over phase).

2.2 Light curves

The early light curves are shown in Fig. 4. Since SN 2002cv is not visible in the *B* band, the phase is relative to the epoch of the
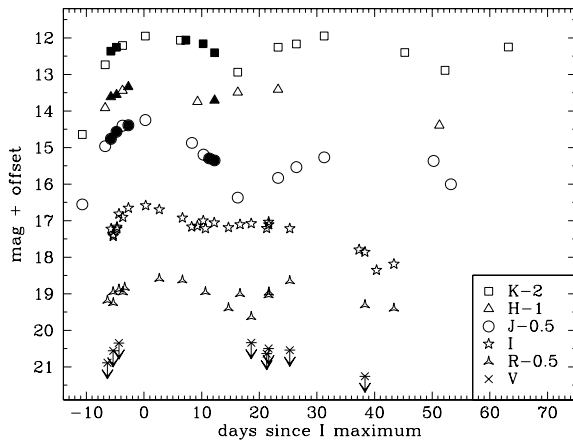

Figure 4. S-corrected *VRIJHK* light curves of SN 2002cv during the first weeks post-explosion. The original data measurements by Di Paola et al. (2002) (AZTDP in Table 5) are marked as the filled symbols. The light curves have been shifted by the amount shown in the legend.

first *I*-band maximum, which occurred on 2002 May 20.6 (JD = 245 2415.1 ± 0.2).

The light curves have good sampling from −10 to +64 d after *I* maximum, except in *V* where only upper limits could be measured. SN 2002cv was discovered in the *JK* bands about 10.7 d before the *I* maximum, making these measurements among the earliest NIR observations available for an SN Ia.

A secondary maximum in the red and NIR light curves is easily visible, which is typical of SNe Ia and confirms the early classification of SN 2002cv. We remind the reader that no definite classification was assigned to SN 2002cv because of the lack of clear spectral features bluewards of 6000 Å. Another typical SN Ia signature is the first *I* maximum occurring before those in *R* and the NIR (e.g. Contardo, Leibundgut & Vacca 2000).

The *R*-band light curve presents a pronounced secondary maximum, which is unusual for an SN Ia. This is probably due to the high reddening suffered by SN 2002cv, which shifts the effective wavelength of the *R* bandpass to the red, mimicking the *I* light curve of an unreddened SN Ia. In fact, we verified that, given the SN 2002cv spectrum, the actual effective wavelength shifts from ∼6550 to ∼7100 Å, which leads to a difference in magnitude up to 0.3, mainly visible at the phase of the secondary maximum. This effect is negligible in the *IJHK* bands.

We note also that the post-maximum decline of the *J* light curve is much steeper than that in the *I* band, showing a pronounced *J* minimum around day +16. On the other hand, a shallow *H* minimum occurs a few days earlier than those in *J* and *K*. All these features, except the broad *K* peak, are typical of SNe Ia (Meikle 2000).

For comparison, in Fig. 5 we plot the *I* light curves of three nearby SNe Ia (see Section 5 for more information) having different
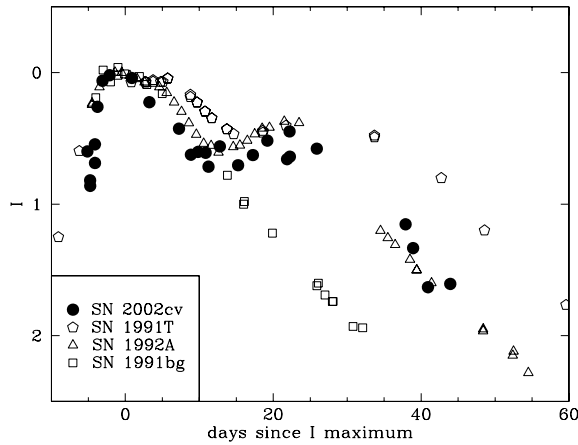
Figure 5. Comparison between the *I*-band light curve of SN 2002cv and three other SNe Ia with different $\Delta m_{15}(B)$ values: SN 1991T [$\Delta m_{15}(B) = 0.94$ mag], SN 1991bg [$\Delta m_{15}(B) = 1.94$ mag] and SN 1992A [$\Delta m_{15}(B) = 1.47$ mag] normalized to the *I* maximum. See Table 9 for more information about these SNe.

Figure 6. Colour evolution of SN 2002cv compared with those of SNe 2002bo (Benetti et al. 2004; Krisciunas et al. 2004b), 2001bt, 2001cz (Krisciunas et al. 2004b), 1999ee, 2001ba (Krisciunas et al. 2004a) and 2001el (Krisciunas et al. 2003). The best fit is obtained for a reddening $A_V = 8.99 \pm 0.30$ mag and total-to-selective extinction ratio $R_V = 1.97 \pm 0.30$.

Figure 7. Colour evolution of SN 2002cv compared with that of SN 2001el (Type Ia, Krisciunas et al. 2003), SN 2004aw (Type Ic, Taubenberger et al. 2006) and SN 2005cs (Type IIP, Pastorello et al. 2006; Pastorello et al., in preparation). The curves have been dereddened according to the values reported in the mentioned papers.

values of $\Delta m_{15}(B)$: SN 1991T [$\Delta m_{15}(B) = 0.94$ mag], SN 1991bg [$\Delta m_{15}(B) = 1.94$ mag] and SN 1992A [$\Delta m_{15}(B) = 1.47$ mag]. The light curves have been shifted to match the first *I* maximum. The light curve of SN 2002cv is best matched by that of SN 1992A even if in the former the first maximum is slightly narrower. Assuming that the two SNe were also similar in the *B* band, we can assign tentatively to SN 2002cv a value $\Delta m_{15}(B) \approx 1.5$ mag. We obtain a better estimate of $\Delta m_{15}(B)$ in Section 5.3.

2.3 Colour and pseudo-bolometric curves

In Fig. 6, the evolution of the intrinsic ($I - $ NIR) colours for SN 2002cv (corrected for the reddening as discussed in Section 4) is compared with those of a sample of SNe Ia. The colour curves are in general very similar to those of normal SNe Ia such as SN 2001cz (Krisciunas et al. 2004b) or SN 2001el (Krisciunas et al. 2003), but with some differences in $(I - K)_0$.

The good match of the SN 2002cv colour curve with those of other normal SNe Ia is another confirmation of the Type Ia classification of this SN. This is strengthened by the comparison presented in Fig. 7, in which the $(I - J)_0$ curve of SN 2002cv is compared with those of different types of SNe: SN 2001el (Type Ia, Krisciunas et al. 2003), SN 2004aw (Type Ic, Taubenberger et al. 2006) and SN 2005cs (Type IIP, Pastorello et al. 2006; Pastorello et al., in preparation). During the pre-maximum period all curves have similar colours, but thereafter the three SN types follow different patterns, with SN 2002cv turning to the blue, as did SN Ia 2001el.

Fig. 8 shows the 'pseudo-bolometric' luminosity evolution of SN 2002cv derived by integrating the flux in the $RIJHK$[3] bands (with the distance modulus and reddening discussed in Section 4). Total uncertainties were computed taking into account photometry errors, and the uncertainties in reddening and distance. We have also plotted the pseudo-bolometric light curves for SN 2002bo and SN 2004eo. The reddening-corrected bolometric luminosity at maximum is $\log_{10} L(RIJHK) = 42.54 \pm 0.30$ (erg s^{-1}). While the first

Figure 8. Pseudo-bolometric ($RIJHK$) light curve for SN 2002cv (filled squares). The open squares and circles give the pseudo-bolometric ($RIJHK$) light curves for SN 2002bo and SN 2004eo, respectively. Error bars include photometric, reddening, and distance uncertainties.

maximum of SN 2002cv is fainter and narrower than those of the other SNe Ia, its secondary maximum is bright and broad, similar to that of SN 2004eo. This is not unexpected, since an overall similarity between SN 2004eo and SN 1992A was noted by Pastorello et al. (2007b).

It is well known that for SNe Ia around maximum, most of the flux is emitted in the *UBV* bands. From the photometry of other SNe Ia, we can estimate that the integrated flux carried by the *RIJHK* bands is approximately 40 per cent (with a variation of around 10 per cent)

---

[3] We have checked that changing the effective wavelength of the *R* band in the calculation of the bolometric light curve results in differences of 0.1 dex in the luminosity. This was taken into account in the error estimate.
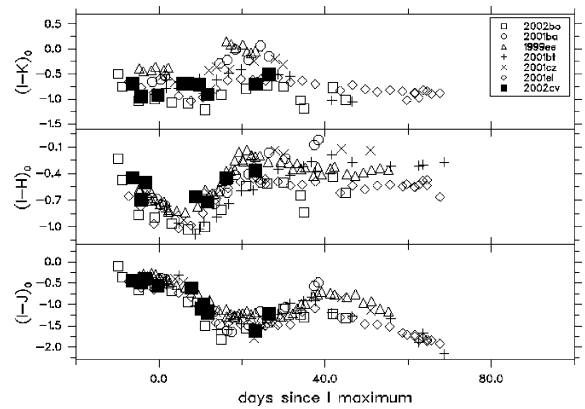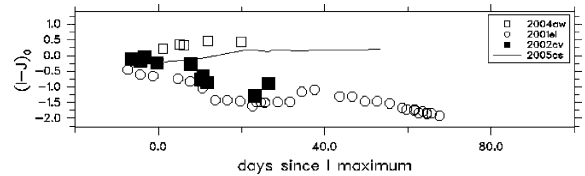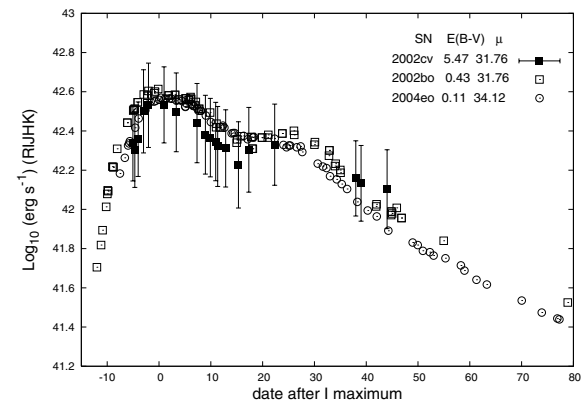
of the integrated 'uvoir' flux from the U through K bands (see also fig. 6 of Contardo et al. 2000). Therefore, we estimate that the total *uvoir* luminosity at maximum of SN 2002cv was $\log_{10} L_{uvoir} = 42.94 \pm 0.60\,(\mathrm{erg\,s^{-1}})$.

Considering that, in general, the B maximum occurs approximately three days after the I maximum, we can derive the epoch of the I secondary maximum relative to B maximum and read the ^{56}Ni mass from fig. 11 of Kasen (2006). In that work, the prominence and timing of the I and J secondary maxima were measured and plotted versus M_{Ni} for I- and J-band models. Kasen (2006) also computed the ^{56}Ni mass of their models considering the absolute maximum and the deep minimum in the J band (fig. 10 of Kasen 2006) and reproduced synthetic model light curves by varying the mass of ^{56}Ni. These models suggest that SN 2002cv has $M(^{56}\mathrm{Ni}) \approx 0.45\,\mathrm{M_\odot}$. This is in good agreement with the ^{56}Ni mass derived from the total *uvoir* luminosity of SN 2002cv at maximum, the Arnett rule (Arnett 1982; Stritzinger & Leibundgut 2005), and a rise time of 19 d, which gives an estimate of the ^{56}Ni mass $M(^{56}\mathrm{Ni}) = 0.44 \pm 0.07\,\mathrm{M_\odot}$. This is also remarkably similar to the ^{56}Ni mass derived by Pastorello et al. (2007b) for SN 2004eo ($0.45\,\mathrm{M_\odot}$).

3 SPECTROSCOPY

3.1 Data reduction

The spectroscopic observations are summarized in Table 6 and the instruments used are as follows.

(i) 1.82-m Copernico telescope of Mt Ekar (Asiago, Italy), equipped with AFOSC (see Section 2.1). Grism#2 (wavelength region 5250–10 300 Å, dispersion 15.67 Å pixel^{-1}, and resolution 38 Å with the 2.1-arcsec slit) was used.

(ii) 3-m Shane reflector (Lick Observatory, Mt Hamilton, California, USA), equipped with Kast (double spectrograph with simultaneous red/blue spectra, wavelength range 3300–10 400 Å).

(iii) 3.6-m ESO/NTT telescope (La Silla, Chile), equipped with EMMI (see Section 2.1). For low-dispersion spectroscopy, grism#2 (wavelength range 3800–9700 Å, dispersion 1.74 Å pixel^{-1}) was used.

(iv) 3.8-m UKIRT (Mauna Kea, Hawaii, USA), equipped with CGS4 (Cooled Grating Spectrometer Mk 4, 1.22 arcsec pixel^{-1}). The 40 line mm^{-1} grating and the *IJHK* filters (wavelength range 8250–25 100 Å) were used.

(v) 3.6-m ESO/NTT telescope (La Silla, Chile), equipped with SofI (see Section 2.1). The grism GBF (wavelength range 9450–

16 520 Å, dispersion 6.96 Å pixel^{-1}, and resolution $\sim$30 Å) was used.

The spectra were reduced using IRAF and FIGARO (for NIR data) routines. The pre-processing of the spectroscopic data (trimming, bias, overscan, and flat-field correction) was the same as for the imaging. For the NIR spectra, before extraction, the contribution of the night-sky lines was removed from the two-dimensional NIR spectrum, subtracting another two-dimensional spectrum with the target placed in a different position along the slit. The one-dimensional spectra were wavelength-calibrated by comparison with arc-lamp spectra obtained during the same night and with the same instrumental configuration, and flux-calibrated using spectrophotometric standard stars. The zero-point of the wavelength calibration was verified against the bright night-sky emission lines. The standard-star spectra were also used to model and remove the telluric absorption. The absolute flux calibration of the spectra was checked against the photometry and when necessary, the spectra were re-scaled. After that, the typical deviation from photometry is less than 10 per cent in all bands.

3.2 Optical and NIR spectra

SN 2002cv was a faint target, especially in the optical: we were able to secure only four spectra in the optical and three in the NIR (Table 6).

The sequence of optical spectra of SN 2002cv is shown in Fig. 9. The spectra are distributed from -4.7 to $+25.4$ d relative to the I-band maximum. Spectra are truncated below 5000 Å because at shorter wavelengths no significant signal from the SN was detected. The most notable feature of the optical spectra is the very red continuum, with almost no sign of individual lines except for the Ca II NIR triplet ($\sim$8500 Å), which is clearly seen two weeks after maximum. In the last spectra, there might also be evidence of the Si II absorption at $\sim$6350 Å.

The NIR spectra of SN 2002cv are shown in Fig. 10. The spectral evolution is typical of SNe Ia. The earliest two spectra are dominated by the continuum. The spectrum at phase $+2.2$ d shows a weak feature with P Cygni profile at about 10 900 Å (rest wavelength) possibly due to Mg II (Wheeler et al. 1998). Weak emission is also visible at 20 500 Å on day $+3.2$, perhaps due to Co II lines (Marion et al. 2003). In the $+26.4$ d spectrum, several individual broad features are remarkably strong. In particular, a prominent absorption at $\sim$12 300 Å (Marion et al. 2003) is attributed to Fe II. At about 15 000 Å, SN 2002cv shows the rapid flux turnover also

Table 6. Optical and NIR spectroscopic observations of SN 2002cv.

UT date	JD (2 400 000.00)	Phase^a (d)	Grism/Grating	Range (Å)	Instrument
15/05/02	524 10.42	-4.7	gm2	5250–10 300	Ekar
19/05/02	524 13.77	-1.3	^{b}	3300–10 400	Shane
8/06/02	524 33.75	$+18.7$	^{b}	3300–10 400	Shane
15/06/02	524 40.52	$+25.4$	gm2	3900–9700	EMMI
22/05/02	524 17.25	$+2.2$	gmij	8250–13 500	UKIRT
23/05/02	524 18.25	$+3.2$	gmk	19800–25 100	UKIRT
15/06/02	524 41.49	$+26.4$	gmB	9450–16 512	SofI

^{a}Relative to I_{max} (JD = 2 452 415.09). ^{b}Grating 300/7500 + grism 600/4310.
Notes. Ekar = 1.82-m Copernico Telescope + AFOSC; Shane = 3-m Shane reflector + Kast dual spectrograph; EMMI = 3.6-m ESO NTT plus; EMMI; UKIRT = 3.8-m United Kingdom Infrared Telescope + CGS4; SofI = 3.6-m ESO NTT + SofI.
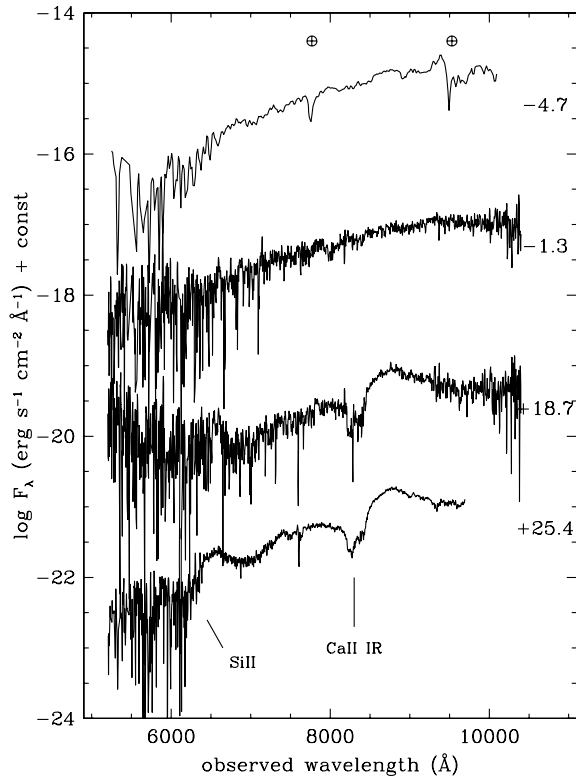
Figure 9. Optical spectra of SN 2002cv, not corrected for reddening. The ordinate refers to the first spectrum and the others have been shifted downwards by arbitrary amounts (0, −1, −3 and −5.5 from the top to bottom panel). Epochs (days) relative to *I* max are given at the right-hand side.
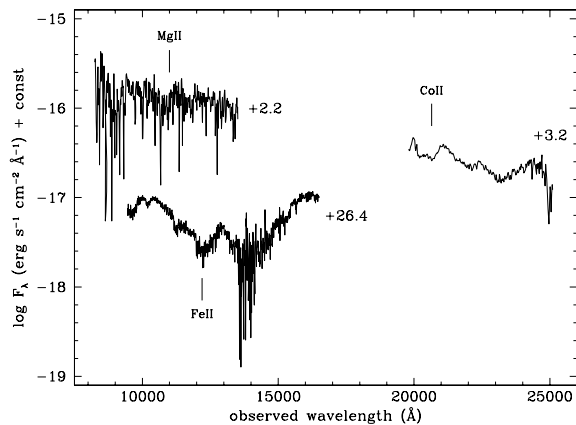

Figure 10. NIR spectra of SN 2002cv, not corrected for reddening. The ordinate refers to the first spectrum and the others have been shifted downwards by arbitrary amounts (0, −1 and −2.5 from the top to bottom panel). Epochs are given at the right-hand side.

observed in other SNe Ia. According to Wheeler et al. (1998) and Marion et al. (2003), this occurs because the region between 11 000 and 15 000 Å has fewer blends of iron-group lines compared to adjacent wavelengths.

Fig. 11 shows the combined, nearly coeval optical and NIR spectra of SN 2002cv (NTT+EMMI at +25.4 d and NTT+SofI at phase +26.4 d) compared with similar-age spectra of SN 2004eo (SN Ia, Pastorello et al. 2007b), SN 2004aw (SN Ic, Taubenberger et al.
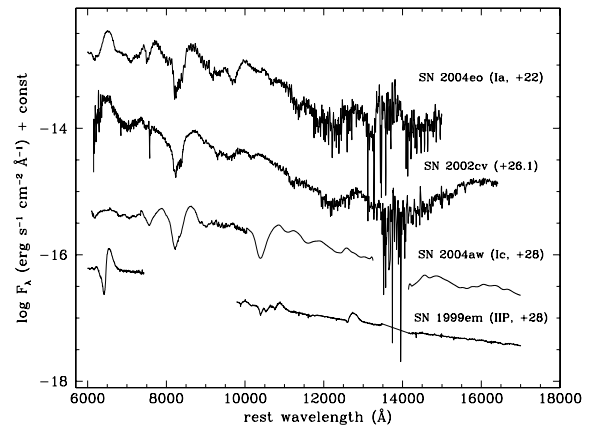
Figure 11. Comparison between the combined optical and NIR spectra of SN 2002cv at +25.4 and +26.4 d after *I* maximum (respectively) with those of SN 2004eo (SN Ia, Pastorello et al. 2007b), SN 2004aw (SN Ic, Taubenberger et al. 2006) and SN 1999em (SN IIP, Hamuy et al. 2001; Leonard et al. 2002). All of the spectra have been corrected for redshift and reddening.
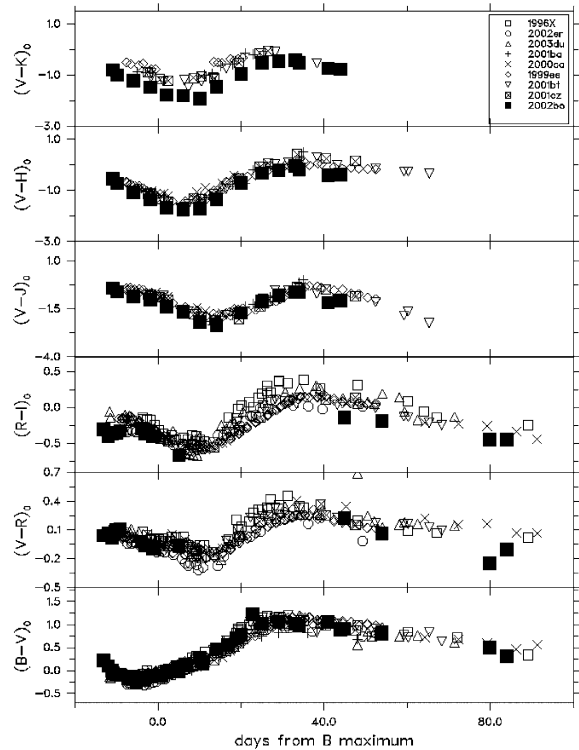

Figure 12. The same as in Fig. 6 but for SN 2002bo. The best match of the curves is obtained for $A_V = 1.50 \pm 0.30$ mag and $R_V = 2.99 \pm 0.30$.

2006) and SN 1999em[4] (SN IIP, Hamuy et al. 2001; Leonard et al. 2002). This comparison definitely confirms that SN 2002cv is an SN Ia (see, in particular, the overall similarity to SN 2004eo). Moreover, the pronounced P Cygni profile of Hα and Pβ of SNe II (SN 1999em, 6562.8 and 12 818 Å), and the He I and C I around 10 830 Å of SNe Ic (SN 2004aw), is are present in SN 2002cv.

---

[4] The SN 1999em spectra were downloaded from SUSPECT (the Online Supernova Spectrum Archive): http://bruford.nhn.ou.edu/suspect/index1.html.

Table 7. Basic input data to find the values of A_V, R_V and μ by maximum-likelihood estimation.

Filter	$m^{02\text{cv}\ a}_{\lambda,\text{max}}$	$M^{02\text{cv}\ b}_{\lambda,\text{max}}$	$m^{02\text{bo}\ c}_{\lambda,\text{max}}$	$M^{02\text{bo}\ d}_{\lambda,\text{max}}$	$A_{\lambda,\text{Gal}}$
B	–	–	14.04 ± 0.10	-19.27 ± 0.04	0.102
V	–	–	13.58 ± 0.10	-19.20 ± 0.04	0.078
R	19.08 ± 0.20	-19.04 ± 0.13	13.49 ± 0.10	-19.21 ± 0.04	0.063
I	16.57 ± 0.10	-18.79 ± 0.12	13.52 ± 0.10	-18.94 ± 0.04	0.046
J	14.75 ± 0.03	-18.61 ± 0.13	–	–	0.022
H	14.34 ± 0.01	-18.28 ± 0.15	–	–	0.015
K	13.91 ± 0.04	-18.44 ± 0.14	–	–	0.009

[a]Observed magnitudes at maximum of SN 2002cv for each band (see Section 5.3). [b]Adopted absolute magnitudes of SN 2002cv. For R and I see Section 5.3; for J, H and K we used the mean absolute magnitudes given by Krisciunas et al. (2004b). [c]Observed magnitudes at maximum of SN 2002bo (Benetti et al. 2004). [d]Adopted absolute magnitudes of SN 2002bo (Prieto et al. 2006).
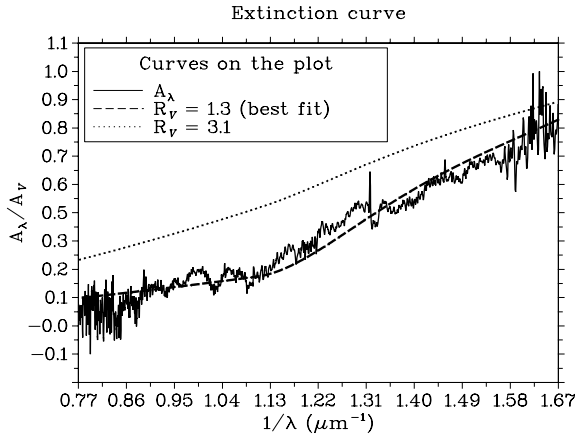

Figure 13. Best fit of the observed extinction law (A_λ/A_V) with the theoretical CCM laws (dashed line). In the example, the extinction curve of SN 2002cv was obtained by dividing the spectrum of SN 2002cv on day +26 by that of SN 2004eo from 6000 to 12 500 Å. For comparison, we also plot the CCM extinction curve for $R_V = 3.1$ (dotted line). From the average of 12 comparisons using four different SNe as templates (see the text for more information), we obtained $A_{V,\text{host}} = 8.17 \pm 0.57$ mag and $R_V = 1.52 \pm 0.11$.

4 THE REDDENING ESTIMATE

We mentioned in the Introduction section that extinction can be the dominant source of error in the spectrophotometric calibration of SNe Ia. This is especially true for SN 2002cv because of the very high extinction.

Di Paola et al. (2002) derived an estimate of the extinction of SN 2002cv after assuming typical J, H and K absolute magnitudes for SNe Ia, as follows:

$$A_\lambda = m_\lambda - M_\lambda - \mu. \tag{1}$$

Using a standard extinction law, these NIR estimates were converted to an average $A_V = 7.90 \pm 0.90$ mag. However, we found that using this approach for different bands gives values of A_V which are inconsistent, with progressively lower values moving from red to blue bands. As in other similar cases (e.g. Elias-Rosa et al. 2006; Krisciunas et al. 2006), the simplest explanation is that R_V has a value smaller than the standard 3.1.

To derive consistent estimates of both A_V and R_V, we adopt three different procedures, all based on the comparison of the SED and the luminosity of SN 2002cv with those of other standard SNe Ia.

(i) We performed a simultaneous match of the $I - J, I - H$ and $I - K$ colour curves of SN 2002cv with those of other normal SNe Ia (Fig. 6). As in the case of SN 2003cg (Elias-Rosa et al. 2006),

it turns out that the best fit requires a value of R_V smaller than the canonical one. The best match is for $A_V = 8.99 \pm 0.30$ mag and $R_V = 1.97 \pm 0.30$.

It is interesting to apply the same methods to SN 2002bo, which exploded in the same host galaxy as SN 2002cv. In this case, we can make use of more colours, namely $B - V, V - R, R - I, V - J, V - H$ and $V - K$. Matching the colours of SN 2002bo to those of normal SNe Ia (Fig. 12) gives a best fit of $A_V = 1.50 \pm 0.30$ mag and $R_V = 2.99 \pm 0.30$. This dust extinction law is consistent with the average one in the Galaxy. However, we note in Fig. 12 that the $V - \text{NIR}$ colour curves of SN 2002bo do not fit those of normal SNe Ia well. This was already noted by Krisciunas et al. (2004a) and attributed to a real peculiarity in the SED of this SN.

Since R_V is related to the grain size, the different extinction laws found for SN 2002bo and SN 2002cv show that in NGC 3190, dust having different average properties coexists. This is an important fact but at the same time not surprising, since in the Galaxy we also observe regions with very different values of R_V (Fitzpatrick 2004; Geminale & Popowski 2005).

(ii) The observed extinction curve is derived by comparing the observed optical (>6000 Å) and NIR SED of SN 2002cv with those of unreddened SNe Ia, at similar epochs. The spectra used for this comparison were previously corrected for redshift and Galactic reddening, and scaled to the distance of SN 2002cv (an example is shown in Fig. 13). This method was applied by Elias-Rosa et al. (2006) to derive the extinction law to SN 2003cg.

We used as templates the spectra of SN 1992A, SN 1994D, SN 1996X and SN 2004eo (see Section 5 for more details about these SNe), comparing a total of 12 pairs of spectra at different epochs and obtaining in each case an estimate of A_V and R_V. The average values are $A_{V,\text{host}} = 8.17 \pm 0.57$ mag and $R_V = 1.52 \pm 0.11$.

(iii) Exploiting the fact that SN 2002bo exploded in the same galaxy as SN 2002cv, we performed a multidimensional maximum-likelihood estimate[5] to find the values of A_V, R_V and μ that give the best match to the measurements in columns 3 and 5 of Table 7 according to the relation

$$M'_\lambda(A_V, R_V, \mu) = m_\lambda - \mu - A_{\lambda,\text{Gal}} - \left[A_V \left(a_\lambda + \frac{b_\lambda}{R_V} \right) \right]_{\text{host}}, \tag{2}$$

where a_λ and b_λ are wavelength-dependent coefficients given by Cardelli, Clayton & Mathis (1989, hereafter CCM). Here, we

[5] The maximum-likelihood method is the procedure of finding the value of one or more parameters for a given statistic which makes the known likelihood distribution a maximum (Myung 2003).
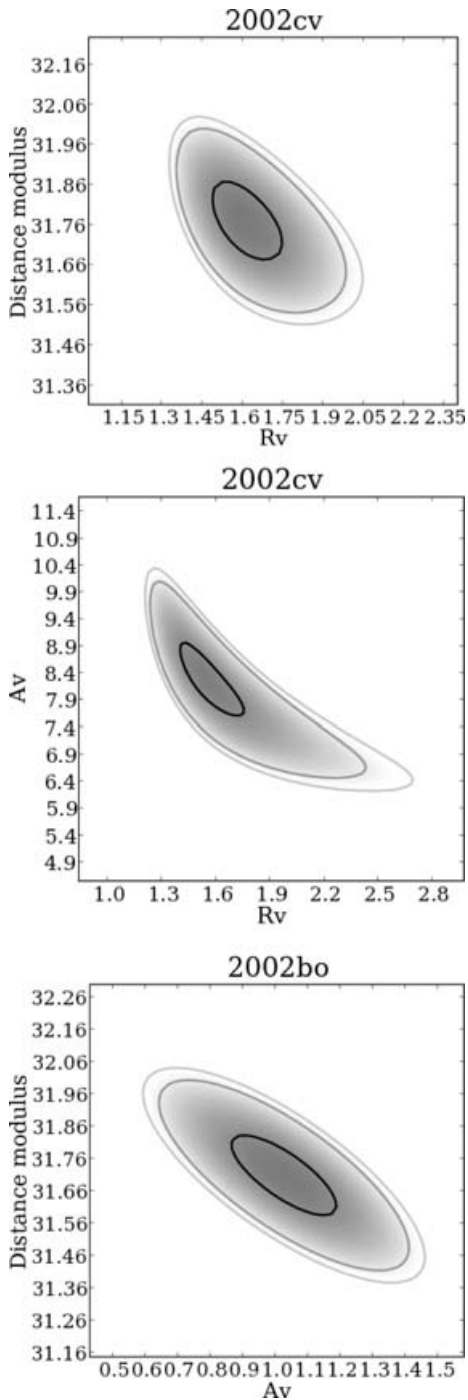
Figure 14. Multidimensional maximum-likelihood estimates to derive A_V and R_V towards SN 2002cv and SN 2002bo along with the host-galaxy distance. Each contour corresponds to 3σ (outer curve), 2σ (middle curve) and 1σ (inner curve). The values found were $A_V = 8.40 \pm 0.35$ mag and $R_V = 1.60 \pm 0.10$ for SN 2002cv, $A_V = 1.00 \pm 0.10$ mag for SN 2002bo, and $\mu = 31.76 \pm 0.07$ mag.

remind the reader of the shift in the R effective wavelength due to the high extinction of SN 2002cv (see Section 2.2). This effect is smaller at maximum light than in the later phases, and hence we included the R-band measurements in our fit (Table 7). For a simultaneous fit to the data of the two SNe, the free parameters are $A_{V,02cv}$, $A_{V,02bo}$, $R_{V,02cv}$, $R_{V,02bo}$ and $\mu = \mu_{02cv} = \mu_{02bo}$.

Table 8. Values of A_V and R_V derived from different methods.

Method	$A_{V,\mathrm{host}}$ (mag)	R_V
Colour evolution	8.99 ± 0.30	1.97 ± 0.30
Comparison of CCM	8.17 ± 0.57	1.52 ± 0.11
Multidimensional	8.40 ± 0.35	1.60 ± 0.10

Actually, following the results of method (i), we fixed for SN 2002bo a standard value $R_V = 3.1$. Also, due to the different $V - $ NIR colour curves of SN 2002bo [see Krisciunas et al. 2004a and method (i)], we did not include the NIR bands of this SN in our fit.

Fig. 14 shows the 1, 2 and 3σ confidence levels projected in the planes of selected parameter pairs. The uncertainty in R_V and A_V can be read from the 1σ contour. The maximum-likelihood test gives the following results: $A_V = 8.40 \pm 0.35$ mag, $R_V = 1.60 \pm 0.10$ for SN 2002cv, $A_V = 1.00 \pm 0.10$ mag for SN 2002bo, and a distance modulus of $\mu = 31.76 \pm 0.07$ mag for NGC 3190.

We note that the value of μ found here is in excellent agreement with $\mu = 31.77$ mag, the distance modulus derived using the relative distance of NGC 3190 from the Virgo cluster (1.48 mag, Kraan-Korteweg 1986), and assuming a Virgo cluster distance of 15.3 Mpc (Freedman et al. 2001). An alternative estimate of the distance is obtained considering that NGC 3190 is a member of the Leo III group (García 1993); the surface brightness fluctuation (Tonry et al. 2001a) distance of another possible member of the group, NGC 3226, is $\mu = 31.86 \pm 0.24$ mag (Krisciunas et al. 2004b). This is also in good agreement with our estimate above, which we hereafter adopt.

In summary, the A_V and R_V estimates obtained with the three different procedures are listed in Table 8. The weighted averages of these values are $A_V = 8.66 \pm 0.21$ mag and $R_V = 1.59 \pm 0.07$.

Including the Galactic extinction component, $E(B - V)_{\mathrm{Gal}} = 0.025$ mag (Schlegel, Finkbeiner & Davis 1998), the total extinction suffered by SN 2002cv is $A_{V\mathrm{tot}} = 8.74 \pm 0.21$ mag, making SN 2002cv one of the most highly extinguished SNe Ia ever observed.

With regard to the extinction law, we stress that all three methods give a low value of R_V. The small value of R_V obtained for this source, which is deeply embedded in a dust lane, appears consistent with the scenario proposed by Goudfrooij et al. (1994) and Patil et al. (2007), who suggest that the observed dust-grain size in the host-galaxy dust lanes may be altered by different mechanisms, such as destruction of grains due to sputtering in SN blast waves, grain–grain collisions, or sputtering by warm and hot thermal ions (Goudfrooij et al. 1994). A possible different mechanism for producing small dust grains is erosion by the SN radiation field (Whittet 1992). In this case, the dust must be located close to the SN, possibly even originating in the progenitor evolution.

We should mention, however, the alternative explanation for the small apparent value of R_V proposed by Wang (2005), which invokes the effect of a light echo from circumstellar dust. In this scenario, the physical properties of the dust are much less important than its distribution in the immediate neighbourhood of SNe Ia.

In conclusion, SNe Ia can be a very useful tool for studying the properties of dust in distant galaxies.

5 PHOTOMETRIC PARAMETERS

The parameters characterizing the photometric behaviour of SNe Ia are usually derived from B and V light curves. For SN 2002cv, the B and V bands are heavily extinguished and no measurements were

obtained (we measured only upper limits in the *V* band). Hence, to characterize this SN with respect to other events we will seek general correlations between blue and red light curve parameters of SNe Ia.

5.1 *VRI* decline rates versus $\Delta m_{15}(B)$

Hamuy et al. (1996c), using a sample of seven SNe Ia, showed a strong correlation between $\Delta m_{15}(B)$ and other light curve parameters, namely $\Delta m_{60}(B)$, $\Delta m_{20}(V)$, $\Delta m_{60}(V)$ and $\Delta m_{60}(I)$. They also found that for the *I* band, the time-interval between the minimum and the secondary maximum is greater for the slowly declining SNe Ia.

Here, we extend the statistics of Hamuy et al. (1996c) to a sample of 20 SNe Ia (Table 9) spanning a range in $\Delta m_{15}(B)$ between 0.90 and 1.94 mag. For each SN, we obtained the epoch and magnitude of the maximum light in the V, R and *I* bands, and measured the decay in the first 15, 20, 40 and 60 d after maximum in each band. See Fig. 15 for a graphical description of these parameters.

We note that the decline rates presented here are not corrected for extinction. Phillips et al. (1999) showed that $\Delta m_{15}(B)$ has a weak dependence on reddening. To check if a similar correction was required in the other bands, we measured $\Delta m_{15}(B)$, the decline rates Δm in other bands, as well as $\Delta t_{\mathrm{max}}(I)$ using the spectrophotometry of three SNe Ia (SN 1994D, SN 1996X and SN 2004eo). The measurements were performed for (i) the unreddened spectra and (ii) the spectra reddened by the Galactic and host-galaxy extinction with the laws found for SN 2002cv (see Section 4). We confirm the correction for $\Delta m_{15}(B)$ given by Phillips et al. (1999), but the corrections for the *I*-band parameters turned out to be negligible.

Fig. 16 (bottom panel) shows the decline rates of the V, R and *I* light curves versus $\Delta m_{15}(B)$. The correlations between the different

decline rates with $\Delta m_{15}(B)$ are similar to those found by Hamuy et al. (1996c).

The behaviour of the *R*-band decline rates (Fig. 16, middle panel) is different according to the different intervals considered. While there are no correlations between $\Delta m_{15}(B)$ and $\Delta m_{15}(R)$ or $\Delta m_{20}(R)$ except for rapidly declining SNe (SN 1991bg), we find a stronger correlation with $\Delta m_{60}(R)$. This behaviour of the decline rates is probably due to the change in opacity and concentration of iron-peak elements in the central regions during these first days (Kasen 2006), which produce the secondary maximum. According to this model, an SN Ia with homogeneous abundance distribution shows red light curves in which the first and second maxima are indistinguishable. This could be the case for SN 1991bg, which has no secondary maximum and exhibits fast decline in the *B* band and in redder bands.

In Fig. 16 (top panel), we also compare the parameters measured for the *I*-band light curve with $\Delta m_{15}(B)$. While it appears that $\Delta m_{15}(I)$ remains constant, there is a clear correlation between $\Delta m_{40}(I)$, $\Delta m_{60}(I)$ and $\Delta m_{15}(B)$.

In the *I* band, the secondary maxima are very pronounced, as well as in the J, H and K light curves. The strength and phase of the secondary maximum are found to correlate with $\Delta m_{15}(B)$, being more prominent and delayed in luminous SNe Ia (Hamuy et al. 1996c; Nobili et al. 2005). We measured the magnitude difference ΔI_{max} and time-interval $\Delta t_{\mathrm{max}}(I)$ between the primary and secondary peaks in the *I*-band light curve for the SNe of our sample (see Fig. 17), and compared them with $\Delta m_{15}(B)$. Note that SNe with $\Delta m_{15}(B) \geqslant$ 1.8 mag, similar to SN 1991bg, are not included in the diagram because their *I* light curves do not show a secondary maximum.

While ΔI_{max} shows no clear correlation with $\Delta m_{15}(B)$ (Fig. 17, bottom panel), the correlation between $\Delta t_{\mathrm{max}}(I)$ and $\Delta m_{15}(B)$ is tight

Table 9. Main parameters for the SN Ia sample.

SN	$\Delta m_{15}(B)_{\mathrm{obs}}$	JD(I_{max}) (2 400 000.00)	I_{max}	$\Delta m_{40}(I)_{\mathrm{obs}}$	$\Delta t_{\mathrm{max}}(I)$	μ	$A_{I,\mathrm{tot}}$[a]	Sources
SN 1992bc	0.90(0.05)	48 910.84(0.50)	15.56(0.05)	0.98(0.06)	33.13(1.13)	34.56	0.04	0, 1, 2, 3
SN 1991T	0.94(0.05)	48 371.60(0.50)	11.62(0.04)	0.69(0.01)	27.75(0.51)	30.74	0.33	0, 1, 2, 4, 5, 6, 7
SN 2003du	1.02(0.05)	52 764.92(0.50)	13.83(0.02)	0.97(0.03)	29.78(0.71)	32.42	0.01	0, 1, 8
SN 1990N	1.05(0.05)	48 080.70(0.50)	12.95(0.02)	–	28.86(1.05)	31.07	0.10	0, 1, 2, 6
SN 1992al	1.09(0.05)	48 836.86(0.50)	14.93(0.04)	1.02(0.02)	27.50(0.71)	33.82	0.05	0, 1, 2, 3
SN 2005cf	1.11(0.03)	53 532.00(0.50)	13.70(0.03)	0.96(0.03)	29.60(0.55)	32.19	0.14	0, 1, 9
SN 2003cg	1.12(0.05)	52 728.22(0.50)	13.82(0.04)	1.13(0.04)	28.08(0.71)	31.61	1.14	0, 1, 10
SN 2001el	1.13(0.05)	52 181.43(1.00)	12.81(0.06)	0.97(0.04)	27.26(1.01)	31.29	0.27[b]	0, 1, 2, 11
SN 2002bo	1.17(0.05)	52 355.50(1.00)	13.49(0.10)	0.98(0.10)	27.94(1.00)	31.77	0.56	0, 1, 12, 13
SN 1995E	1.19(0.05)	49 771.00(0.50)	15.33(0.05)	1.01(0.05)	–	33.43	1.01	0, 1, 2, 14
SN 1998dh	1.23(0.17)	51 029.32(0.50)	14.10(0.05)	1.21(0.05)	27.50(0.69)	32.92	0.31	0, 1, 2, 15
SN 1994D	1.31(0.05)	49 428.50(1.00)	12.11(0.05)	1.31(0.06)	25.02(1.01)	31.14	0.04	0, 1, 16, 17, 18, 19
SN 1996X	1.32(0.05)	50 188.00(1.00)	13.39(0.01)	1.10(0.02)	27.71(1.05)	32.17	0.10	0, 1, 14, 20
SN 2002er	1.33(0.04)	52 523.56(0.50)	14.49(0.05)	1.40(0.09)	26.14(0.71)	32.90	0.53	0, 1, 21
SN 1997E	1.39(0.06)	50 466.19(0.50)	15.46(0.05)	1.44(0.07)	22.78(1.41)	33.72	0.28	0, 1, 2, 15
SN 2004eo	1.45(0.04)	53 276.30(1.00)	15.36(0.04)	1.26(0.04)	24.13(1.03)	34.12	0.21	0, 1, 22
SN 1992A	1.47(0.05)	48 638.00(0.50)	12.80(0.04)	1.46(0.05)	22.08(0.56)	31.41[c]	0.09	0, 1, 2, 7, 23
SN 2000cn	1.58(0.12)	51 706.93(0.50)	16.63(0.05)	–	–	34.93	0.16	0, 1, 2, 15
SN 1992bo	1.69(0.05)	48 984.94(0.50)	15.95(0.05)	1.68(0.05)	20.00(0.71)	34.28	0.08	0, 1, 2, 3
SN 1991bg	1.94(0.05)	48 608.60(1.00)	13.51(0.05)	2.42(0.05)	–	31.32	0.06	0, 1, 2, 24, 25, 26, 27

[a] $A_{I,\mathrm{Gal}} + A_{I,\mathrm{host}}$. [b] $E(B-V)_{\mathrm{host}} = 0.18$ mag, with $R_V = 2.88$. [c] Average μ from different sources.

Notes. 0 = This work; 1 = LEDA; 2 = Reindl et al. (2005); 3 = Hamuy et al. (1996b); 4 = Schmidt et al. (1994); 5 = Cappellaro et al. (1997); 6 = Lira et al. (1998); 7 = Altavilla et al. (2004); 8 = Stanishev et al. (2007); 9 = Pastorello et al. (2007a); 10 = Elias-Rosa et al. (2006); 11 = Krisciunas et al. (2003); 12 = Benetti et al. (2004); 13 = Krisciunas et al. (2004a); 14 = Riess et al. (1999); 15 = Jha et al. (2006); 16 = Richmond et al. (2005); 17 = Tsvetkov & Pavlyuk (1995); 18 = Patat et al. (1996); 19 = Meikle et al. (1996); 20 = Salvo et al. (2001); 21 = Pignata et al. (2004); 22 = Pastorello et al. (2007b); 23 = Suntzeff (1996); 24 = Filippenko et al. (1992b); 25 = Leibundgut et al. (1993); 26 = Turatto et al. (1996); 27 = Tonry et al. (2001b).
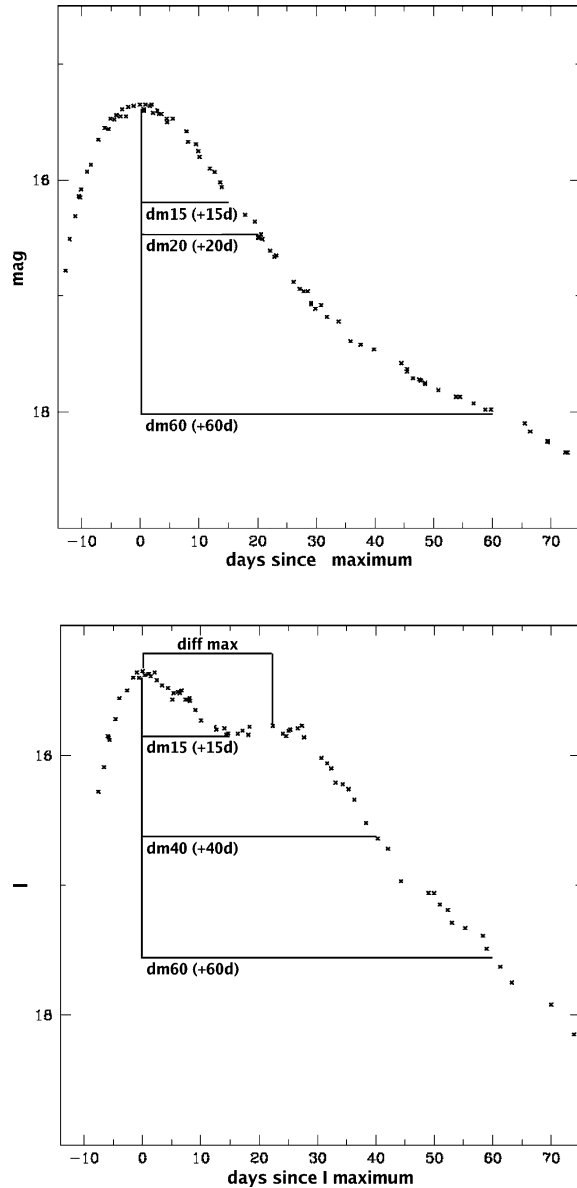
Figure 15. Graphical representation of the parameters defined in Section 5 for generic bands (top panel) and in particular for the *I* band (bottom panel).

(Fig. 17, top panel), with the phase delay of the secondary maximum being longer for slowly declining SNe Ia.

5.2 *I*-band magnitudes and $\Delta m_{15}(B)$

It is well known that the early-time decline rate in the *B*-band light curve of SNe Ia correlates with the luminosity. Since the *B* band is not available for SN 2002cv, we are forced to find alternative indicators to establish the photometric subclass of this SN. In Fig. 5, we have already shown that the *I* light curve shapes of SNe 2002cv and 1992A were similar, so it is likely that they have similar $\Delta m_{15}(B) \approx 1.5$ mag.

In order to obtain a more accurate estimate of $\Delta m_{15}(B)$, we exploit the previously derived correlations with $\Delta m_{40}(I)$ (SN 2002cv was observed until +44.2 d after *I* maximum) and $\Delta t_{\max}(I)$. Using the code developed by Akritas & Bershady (1996) for linear regression analysis, we performed a linear fit to the points in Figs 16 (top panel)
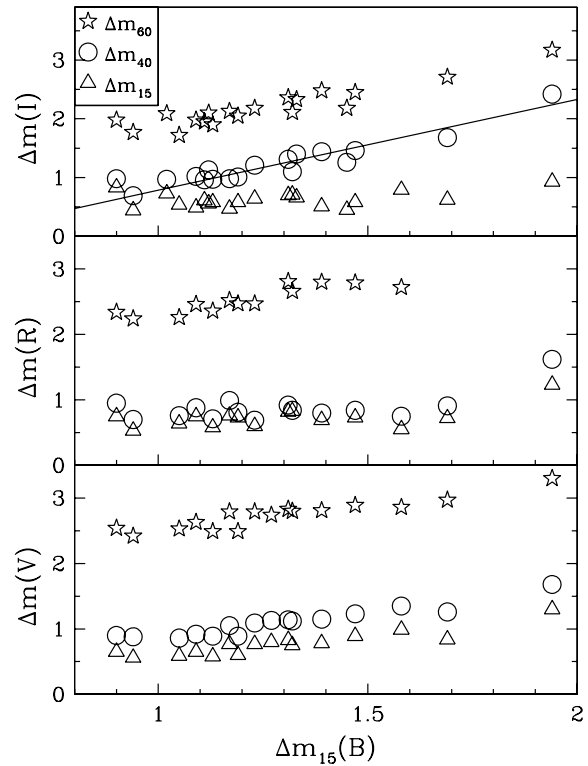
Figure 16. *VRI* light curve decline rates Δm_{15} (triangles), Δm_{20} (circles), and Δm_{60} (stars) versus $\Delta m_{15}(B)_{\mathrm{obs}}$. The straight line is a fit to the $\Delta m_{40}(I)$ points.

and 17 (top panel), obtaining, respectively,

$$\Delta t_{\max}(I) = (48.80 \pm 1.89) - (17.68 \pm 1.52)\,\Delta m_{15}(B) \qquad (3)$$

and

$$\Delta m_{40}(I) = (1.55 \pm 0.17)\,\Delta m_{15}(B) - (0.77 \pm 0.23). \qquad (4)$$

For equation (3), we used 16 SNe Ia and the Pearson correlation coefficient is -0.94; for equation (4), we used 18 SNe Ia and the Pearson correlation coefficient is 0.93.[6]

Since $\Delta m_{15}(B)$ is related to the *B* luminosity of SNe Ia, we could expect a similar relation between $\Delta m_{40}(I)$ and $M_I^{\max}$, the absolute magnitude of the first *I* maximum, and also between $\Delta t_{\max}(I)$ and $M_I^{\max}$. Fig. 18 confirms this expectation, though in both cases the dispersion is high mainly due to the uncertainties in the distance moduli used for computing $M_I^{\max}$.

The linear fits give

$$M_I^{\max} = (-0.05 \pm 0.02) \times \Delta t_{\max}(I) - (17.45 \pm 0.68) \qquad (5)$$

and

$$M_I^{\max} = (1.06 \pm 0.24) \times \Delta m_{40}(I) - (20.14 \pm 0.31). \qquad (6)$$

For the two relations, 15 and 18 SNe Ia were used, and the correlation coefficients are 0.57 and 0.73, respectively.

---

[6] In the fit of $\Delta t_{\max}(I)$ versus $\Delta m_{15}(B)$, we excluded SN 1991T which appears to deviate (as in Hamuy et al. 1996c). Indeed, SN 1991T was an abnormal object with a number of pre-maximum spectroscopic peculiarities (Filippenko et al. 1992a; Phillips et al. 1992).
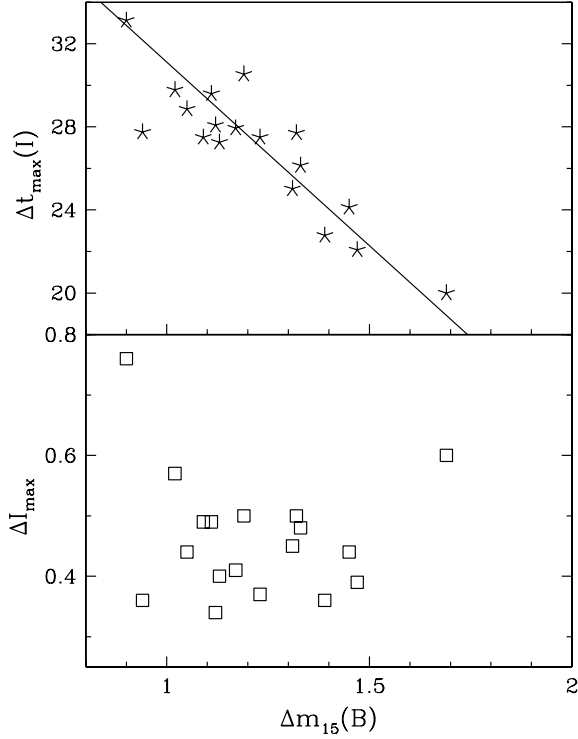
Figure 17. Difference in phase (top panel) and of magnitude (bottom panel) between the primary and secondary maxima of the *I*-band light curve versus $\Delta m_{15}(B)_{\rm obs}$. The straight line is the best fit to the $\Delta t_{\max}(I)$ points.
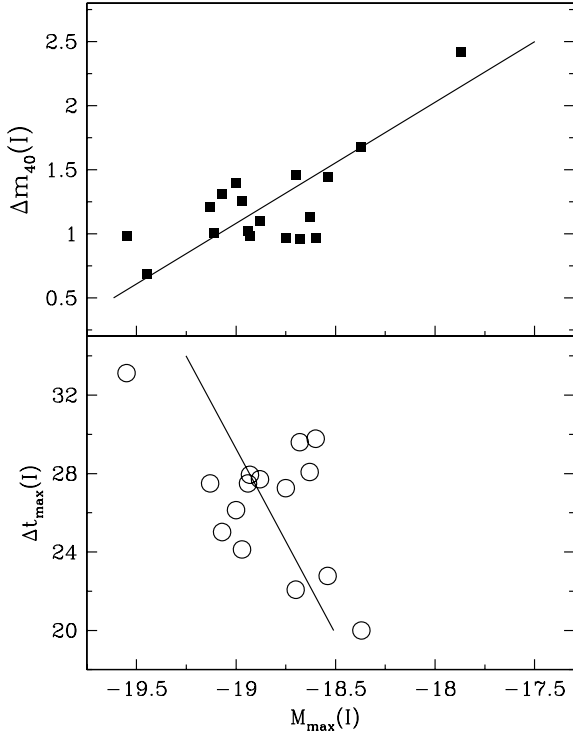

Figure 18. $\Delta m_{40}(I)$ (top panel) and $\Delta t_{\max}(I)$ (bottom panel) versus $M_I^{\max}$, for the SNe Ia of Table 9. The straight lines are the best fits.

Table 10. Main data of SN 2002cv and its host galaxy.

Host-galaxy data	NGC 3190	Reference
α (2000)	$10^{\rm h}18^{\rm m}05\overset{\rm s}{.}60$	1
δ (2000)	$+21°49'55''$	1
Galaxy type	SA(s)a pec	1
B magnitude	12.12	1
$E(B-V)_{\rm Gal}$	0.025	2
$v_{\rm r,helio}$ (km s^{-1})^a	1271	1
μ	31.76 ± 0.07	3
SN data	SN 2002cv	Reference
α (2000)	$10^{\rm h}18^{\rm m}03\overset{\rm s}{.}68$	4
δ (2000)	$+21°50'06''\overset{}{.}20$	4
Offset SN galactic nucleus	18 arcsec west, 10 arcsec north	4
Discovery date (UT)	2002 May 13.7	4
Discovery date (JD)	245 2408.20	4
$E(B-V)_{\rm host}$	5.45 ± 0.28	3
$R_{V\ \rm host}$	1.59 ± 0.07	3
$A_{V\ \rm tot}$	8.74 ± 0.21	3
Date of *I* max (JD)	$245\,2415.09 \pm 0.22$	3
Magnitude and epoch	$V < 19.70$; $\sim$+5.8 (d)	3
at maximum with respect to	$R = 19.08 \pm 0.20$; +3.2 (d)	3
I max		
	$I = 16.57 \pm 0.10$; 0.0 (d)	3
	$J = 14.75 \pm 0.03$; -0.4 (d)	3
	$H = 14.34 \pm 0.01$; -2.0 (d)	3
	$K = 13.91 \pm 0.04$; +1.6 (d)	3
Magnitude and epoch	$I = 17.11 \pm 0.10$; +23.1 (d)	3
of secondary *IJHK*	$J = 15.24 \pm 0.19$; +41.5 (d)	3
max with respect to *I* max	$H = 14.40 \pm 0.11$; +25.9 (d)	3
	$K = 13.88 \pm 0.29$; +35.2 (d)	3
Estimated $\Delta m_{15}(B)_{\rm intr}$	1.46 ± 0.17	3
Absolute magnitude	$M_R^{\max} = -19.05 \pm 0.27$	3
(derived from the distance)	$M_I^{\max} = -18.79 \pm 0.20$	3
	$M_J^{\max} = -18.50 \pm 0.12$	3
	$M_H^{\max} = -18.41 \pm 0.09$	3
	$M_K^{\max} = -18.44 \pm 0.09$	3
$\log_{10} L$ (*RIJHK*)	42.54 ± 0.30 (erg s^{-1})	3
$\log_{10} L_{uvoir}$	42.94 ± 0.60 (erg s^{-1})	3
$M(^{56}{\rm Ni})$	$0.44^{+0.65}_{-0.26}$ (M$_\odot$)	3

^{a}Heliocentric radial velocity.
References. (1) NED; (2) Schlegel et al. (1998); (3) this work; (4) Larionov & Arkharov (2002).

5.3 Main photometric parameters of SN 2002cv

The maximum-light epochs and magnitudes for the different bands, reported in Table 10, were derived by fitting low-order polynomials (lower than 5°) to the light curves. The first *I* maximum is found on JD$(I_{\max}) = 245\,2415.09 \pm 0.22$ (UT 2002 May 20.6) with $I_{\max} = 16.57 \pm 0.10$ mag. The *I*-band secondary maximum occurred $\Delta t_{\max}(I) = 23.06 \pm 0.59$ d later, with magnitude 17.11 ± 0.10. We also measured $\Delta m_{40}(I) = 1.50 \pm 0.32$ mag.

Using equations (3) and (4), we derived an average value $\Delta m_{15}(B) = 1.46 \pm 0.17$, indeed very close to that of SN 1992A and SN 2004eo.

Hereafter, from the measured $\Delta t_{\max}(I)$ and $\Delta m_{40}(I)$, and equations (5) and (6), we derive an estimate of the intrinsic *I* absolute magnitude at maximum for SN 2002cv. The values obtained are $M_I^{\max} = -18.60 \pm 0.84$ and $M_I^{\max} = -18.55 \pm 0.76$ mag, respectively, with a weighted average value of $\langle M_I^{\max}\rangle = -18.57 \pm 0.57$ mag. This magnitude is close to the average value for SNe Ia found by Saha et al. (1999): $\langle M_I^{\max}\rangle = -18.74 \pm 0.03$ mag (scaled to $H_0 = 72$ km s^{-1} Mpc^{-1}).

Table 11. Absolute *I* magnitude of SN 2002cv ($H_0 = 72 \, \text{km s}^{-1} \, \text{Mpc}^{-1}$).

$M_I^{\max}$ (mag)	Method	Reference
-18.79 ± 0.20	distance	This work
-18.57 ± 0.57	Equation (5) and (6)	This work
-18.52 ± 0.20	$M_I^{\max}$ versus $\Delta m_{15}(B)$	Hamuy et al. (1996a)[a]
-18.52 ± 0.28	$M_I^{\max}$ versus $\Delta m_{15}(B)$	Phillips et al. (1999)[b]
-18.79 ± 0.12	$M_I^{\max}$ versus $\Delta m_{15}(B)$	Prieto et al. (2006)[c]

[a]According to the relation given in Table 3 of Hamuy et al. (1996a) (peak luminosity). [b]According to the relation given in table 3 of Phillips et al. (1999). [c]According to the relation given in table 3 of Prieto et al. (2006) (for the complete sample – ALL).

For the *I* band, we can also derive the absolute magnitude through the relation with $\Delta m_{15}(B)$. Using (i) the known relation between the peak luminosity and the $\Delta m_{15}(B)$ of Hamuy et al. (1996a) ('peak subsample' case), (ii) Phillips et al. (1999) (see their table 3), and (iii) Prieto et al. (2006) (complete sample reported in Table 3), scaled to $H_0 = 72 \, \text{km s}^{-1} \, \text{Mpc}^{-1}$, we derived $M_I^{\max}$ quite close to that estimated with our equations (see Table 11). We note that equation (1) with the parameters previously derived provides $M_I^{\max} = -18.79 \pm 0.20$ mag, in excellent agreement with the above estimate within the calculated errors. Note that we consider the absolute magnitudes of SN 2002cv to be those obtained using the distance modulus.

Considering again the Prieto et al. (2006) relation, we obtain an analogous estimate in the *R* band, $M_R^{\max} = -19.04 \pm 0.13$ mag. Hamuy et al. (1996a) and Phillips et al. (1999) do not provide an average relation in the *R* band. As before, by applying equation (1), we obtain a value in excellent agreement, $M_R^{\max} = -19.05 \pm 0.27$ mag.

The NIR absolute magnitudes were estimated from the observed peak magnitude and μ. Their values ($M_J^{\max} = -18.50 \pm 0.12$ mag, $M_H^{\max} = -18.41 \pm 0.09$ mag and $M_K^{\max} = -18.44 \pm 0.09$ mag) are consistent with the average values found by Krisciunas et al. (2004b) within the uncertainties ($M_J^{\max} = -18.61 \pm 0.13$ mag, $M_H^{\max} = -18.28 \pm 0.15$ mag and $M_K^{\max} = -18.44 \pm 0.14$ mag).

6 SUMMARY

We have presented optical and NIR data on SN 2002cv and completed the study of this SN started by Di Paola et al. (2002) including the available data collected worldwide. SN 2002cv exploded in the same galaxy as SN 2002bo, a few months later, and it suffered a very high extinction. The presence of clear secondary maxima in the red and NIR light curves, the colour curves, and the spectral features confirm its early classification as an SN Ia.

We have used different methods to estimate the extinction, adopting in all cases a CCM extinction law with R_V as a free parameter. We obtained $E(B - V) = 5.45 \pm 0.28$ mag and $R_V = 1.59 \pm 0.07$ ($A_{V\text{host}} = 8.66 \pm 0.21$) inside the host galaxy, which give a total absorption $A_V = 8.74 \pm 0.21$ mag. It turns out that SN 2002cv is one of the most-reddened SNe ever observed, and a new entry in the growing list of SNe with a low value of R_V (e.g. SN 1999cl, Krisciunas et al. 2006; SN 2001el, Krisciunas et al. 2007; SN 2002hh, Pozzo et al. 2006; SN 2003cg, Elias-Rosa et al. 2006).

We have constructed empirical relations between $\Delta m_{15}(B)$ and $M_I^{\max}$, the delay in the secondary *I* maximum ($\Delta t_{\max}(I)$), and the decline rate at 40 d in the *I* band ($\Delta m_{40}(I)$). These allow us to derive the luminosity class of an SN Ia, without the use of the unavailable *B*-band data. With these average relations for SN 2002cv, we derive $\Delta m_{15}(B)_{\text{true}} = 1.46 \pm 0.17$ mag and $M_I^{\max} = -18.57 \pm 0.57$ mag, which is marginally fainter than that estimated from the observed peak magnitude and μ: $M_I^{\max} = -18.79 \pm 0.20$ mag.

Since R_V is related to the grain size, the different values of this found for SN 2002bo and SN 2002cv show that in NGC 3190 there is dust with different properties (at least for the two line of sights measured) which are different from those of typical Galactic dust. A possible explanation for the different grain sizes might be the effect of SN radiation on local circumstellar dust or the peculiar physical conditions in dust lanes.

A better understanding of this phenomenon is important both for understanding the nature of the exploding stars and for the calibration of SNe Ia for cosmological use.

REFERENCES

Akritas M. G., Bershady M. A., 1996, ApJ, 470, 706
Alard C., 2000, A&AS, 144, 363
Altavilla G. et al., 2004, MNRAS, 349, 1344
Arnett W. D., 1982, ApJ, 253, 785
Benetti S. et al., 2004, MNRAS, 348, 261
Benetti S. et al., 2005, ApJ, 623, 1011
Branch D. et al., 2006, PASP, 118, 560
Cappellaro E., Mazzali P. A., Benetti S., Danziger I. J., Turatto M., Della Valle M., Patat F., 1997, A&A, 328, 203
Cardelli J. A., Clayton G. C., Mathis J. S., 1989, ApJ, 345, 245 (CCM)
Contardo G., Leibundgut B., Vacca W. D., 2000, A&A, 359, 876
Di Paola A., Larionov V., Arkharov A., Bernardi F., Caratti o Garatti A., Dolci M., Di Carlo E., Valentini G., 2002, A&A, 393, L21

[7] http://www.mpa-garching.mpg.de/~rtn/

Elias-Rosa N. et al., 2006, MNRAS, 369, 1880

Filippenko A. V., 1997, ARA&A, 35, 309

Filippenko A. V., 2005, in Sion E. M., Vennes S., Shipman H. L., eds, White Dwarfs: Cosmological and Galactic Probes. Springer, Dordrecht, p. 97

Filippenko A. V., Porter A. C., Sargent W. L. W., Schneider D. P., 1986, AJ, 92, 1341

Filippenko A. V. et al., 1992a, ApJ, 384, L15

Filippenko A. V. et al., 1992b, AJ, 104, 1543

Filippenko A. V., Chornock R., Foley R. J., Li W., 2002, IAU Circ. 7917

Fitzpatrick E. L., 2004, in Witt A. N., Clayton G. C., Draine B. T., eds, ASP Conf. Ser. Vol. 309, Astrophysics of Dust. Astron. Soc. Pac., San Francisco, p. 57

Freedman W. L. et al., 2001, ApJ, 553, 47

Gamezo V. N., Khokhlov A. M., Oran E. S., 2005, ApJ, 623, 337

Garavini G. et al., 2007, A&A, 471, 527

García A. M., 1993, A&AS, 100, 47

Geminale A., Popowski P., 2005, preprint (astro-ph/0502540)

Goudfrooij P., de Jong T., Hansen L., Nørgaard-Nielsen H. U., 1994, MNRAS, 271, 833

Hachinger S., Mazzali P.A., Benetti S., 2006, MNRAS, 370, 299

Hamuy M., Phillips M. M., Suntzeff N. B., Schommer R. A., Maza J., Aviles R., 1996a, AJ, 112, 2391

Hamuy M. et al., 1996b, AJ, 112, 2408

Hamuy M. et al., 1996c, AJ, 112, 2438

Hamuy M. et al., 2001, ApJ, 558, 615

Hillebrandt W., Niemeyer J. C., 2000, ARA&A, 38, 191

Jha S. et al., 2006, AJ, 131, 527

Kasen D., 2006, ApJ, 649, 939

Kraan-Korteweg R. C., 1986, A&AS, 66, 255

Krisciunas K., Prieto J. L., Garnavich P. M., Riley J. G., Rest A., Stubbs C., McMillan R., 2006, AJ, 131, 1639

Krisciunas K. et al., 2003, AJ, 125, 166

Krisciunas K. et al., 2004a, AJ, 127, 1664

Krisciunas K. et al., 2004b, AJ, 128, 3034

Krisciunas K. et al., 2007, AJ, 133, 58

Landolt A. U., 1992, AJ, 104, 340

Larionov V., Arkharov A., 2002, IAU Circ. 7901

Leibundgut B. et al., 1993, AJ, 105, 301

Leonard D. C. et al., 2002, PASP, 114, 35

Lira P., 1995, MSc. thesis, Univ. Chile

Lira P. et al., 1998, AJ, 115, 234

Marion G. H., Höflich P., Vacca W. D., Wheeler J. C., 2003, ApJ, 591, 316

Mazzali P. A. et al., 2005, ApJ, 623, L37

Mazzali P. A., Röpke F. K., Benetti S., Hillebrandt W., 2007, Sci, 315, 825

Meikle W. P. S., 2000, MNRAS, 314, 782

Meikle P., Mattila S., 2002, IAU Circ. 7911

Meikle W. P. S. et al., 1996, MNRAS, 281, 263

Myung J., 2003, Journal of Mathematical Psychology, 47, 90

Nobili S. et al., 2005, A&A, 437, 789

Nomoto K., Saio H., Kato M., Hachisu I., 2007, ApJ, 663, 1269

Pastorello A. et al., 2006, MNRAS, 370, 1752

Pastorello A. et al., 2007a, MNRAS, 376, 1301

Pastorello A. et al., 2007b, MNRAS, 377, 1531

Patat F., Benetti S., Cappellaro E., Danziger I. J., Della Valle M., Mazzali P. A., Turatto M., 1996, MNRAS, 278, 111

Patat F. et al., 2007, Sci, 317, 924

Patil M. K., Pandey S. K., Sahu D. K., Kembhavi A., 2007, A&A, 461, 103

Perlmutter S. et al., 1997, ApJ, 483, 565

Phillips M. M., Wells L. A., Suntzeff N. B., Hamuy M., Leibundgut B., Kirshner R. P., Foltz C. B., 1992, AJ, 103, 1632

Phillips M. M., Lira P., Suntzeff N. B., Schommer R. A., Hamuy M., Maza J., 1999, AJ, 118, 1766

Pignata G., 2004, PhD thesis, Univ. Padova

Pignata G. et al., 2004, MNRAS, 355, 178

Pozzo M. et al., 2006, MNRAS, 368, 1169

Prieto J. L., Rest A., Suntzeff N. B., 2006, ApJ, 647, 501

Reindl B., Tammann G. A., Sandage A., Saha A., 2005, ApJ, 624, 532

Richmond M. W. et al., 1995, AJ, 109, 2121

Riess A. G., Press W., Kirshner R. P., 1996, ApJ, 473, 88

Riess A. G. et al., 1999, AJ, 117, 707

Röpke F. K., Hillebrandt W., Blinnikov S. I., 2006, in Cruise A. M., Ouwehond L., eds, ESA-SP Vol. 637, Beyond Einstein – Physics for the 21st Century. ESA Publications Division, Noordwijk, p. 16.1

Röpke F. K., Woosley S. E., Hillebrandt W., 2007, ApJ, 660, 1344

Saha A., Sandage A., Tammann G. A., Labhardt L., Macchetto F. D., Panagia N., 1999, ApJ, 522, 802

Salvo M. E., Cappellaro E., Mazzali P. A., Benetti S., Danziger I. J., Patat F., Turatto M., 2001, MNRAS, 321, 254

Savage B. D., Mathis J. S., 1979, Ann. Rev. Astr. Ap., 17, 73

Schlegel D. J., Finkbeiner D. P., Davis M., 1998, ApJ, 500, 525

Schmidt B. P., Kirshner R. P., Leibundgut B., Wells L. A., Porter A. C., Ruiz-Lapuente P., Challis P., Filippenko A. V., 1994, ApJ, 434, 19

Seaton M. J., 1979, MNRAS, 187, 73ᴘ

Stanishev V. et al., 2007, A&A, 469, 645

Stritzinger M., Leibundgut B., 2005, A&A, 431, 423

Stritzinger M. et al., 2002, AJ, 124, 2100

Suntzeff N. B., 1996, in McCray R., Wang Z., eds, Supernovae and Supernova Remnants. Cambridge Univ. Press, Cambridge, p. 41

Suntzeff N. B., 2000, in Holt S. S., Zhang W. W., eds, Cosmic Explosions. Am. Inst. Phys., New York, p. 65

Taubenberger S. et al., 2006, MNRAS, 371, 1459

Tonry J. L., Blakeslee J. P., Ajhar E. A., Dressler A., 2001a, ApJ, 475, 399

Tonry J. L., Dressler A., Blakeslee J. P., Ajhar E. A., Fletcher A. B., Luppino G. A., Metzger M. R., Moore C. B., 2001b, ApJ, 546, 681

Tsvetkov D. Yu., Pavlyuk N. N., 1995, Astron. Lett., 21, 606

Turatto M., Benetti S., Cappellaro E., Danziger I. J., Della Valle M., Gouiffes C., Mazzali P. A., Patat F., 1996, MNRAS, 283, 1

Turatto M., Desidera S., Benetti S., Altavilla G., Pastorello A., Riello M., Cappellaro E., 2002, IAU Circ. 7901

Wang L., 2005, ApJ, 635, L33

Wheeler J. C., Höfflich P., Harkness R. P., Spyromilio J., 1998, ApJ, 496, 908

Whittet D. C. B., 1992, Series in Astronomy and Astrophysics, Dust in the Galactic Environment. IOP Publishing, Bristol & Philadelphia

This paper has been typeset from a TeX/LaTeX file prepared by the author.